Med

CellPress
OPEN ACCESS

Clinical and Translational Article

A pan-cancer clinical platform to predict immunotherapy outcomes and prioritize immuno-oncology combinations in early-phase trials

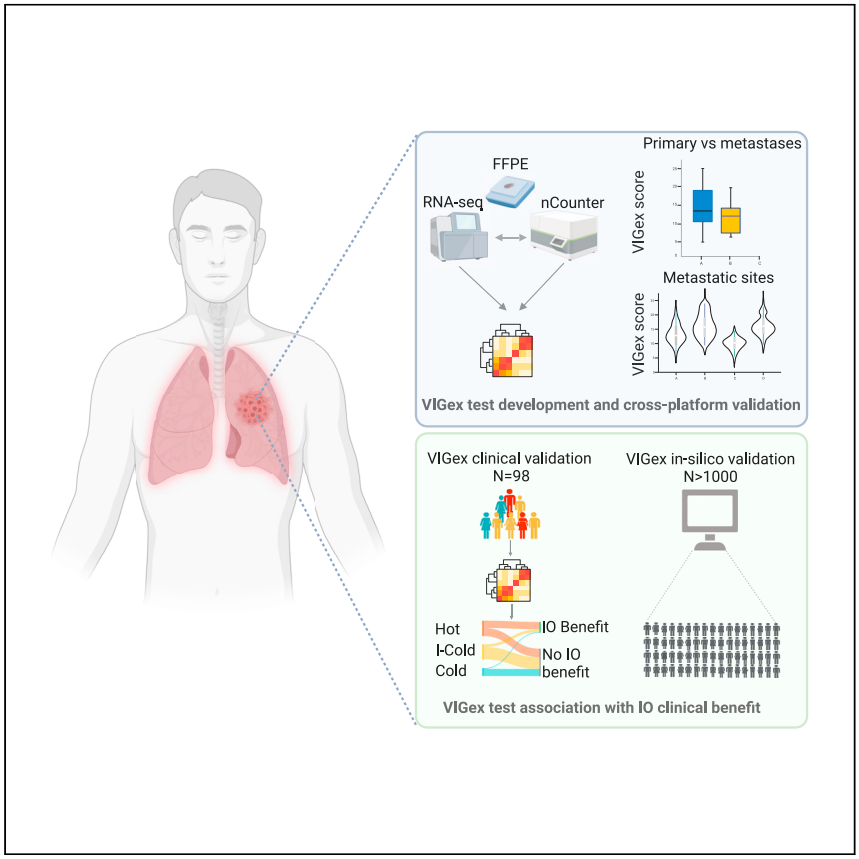

Hernando-Calvo et al. developed VIGex, a pan-cancer immune gene expression signature encompassing 12 immune-related genes, that predicts immunotherapy benefit and prioritizes immunotherapy combinations in early-phase clinical trials.

Alberto Hernando-Calvo, Maria Vila-Casadesús, Yacine Bareche, ..., Josep Tabernero, Elena Garralda, Ana Vivancos

avivancos@vhio.net

Highlights

VIGex is an immune gene expression signature developed in RNA-seq and Nanostring

VIGex classifies samples in hot, intermediate-cold, or cold

VIGex *Z* scores quantify gene expression levels of immunotherapy drug targets

VIGex groups associate with immunotherapy outcomes

Foundational Research

Hernando-Calvo et al., Med 4, 710–727
October 13, 2023
Published by Elsevier Inc.
https://doi.org/10.1016/j.medj.2023.07.006

CellPress
OPEN ACCESS

Med

Clinical and Translational Article

A pan-cancer clinical platform to predict immunotherapy outcomes and prioritize immuno-oncology combinations in early-phase trials

Alberto Hernando-Calvo,[1,2,3,4,12] Maria Vila-Casadesús,[2,12] Yacine Bareche,[5,6] Alberto Gonzalez-Medina,[2] Farnoosh Abbas-Aghababazadeh,[7] Deborah Lo Giacco,[2] Agatha Martin,[2] Omar Saavedra,[1,2] Irene Brana,[1,2] Maria Vieito,[1,2] Roberta Fasani,[2] John Stagg,[5,6] Francesco Mancuso,[2] Benjamin Haibe-Kains,[7,8,9,10,11] Ming Han,[7] Roger Berche,[2] Trevor J. Pugh,[7,8,10] Oriol Mirallas,[1,2] Jose Jimenez,[2] Nadia Saoudi Gonzalez,[1,2] Claudia Valverde,[1,2] Eva Muñoz-Couselo,[1,2] Cristina Suarez,[1,2] Marc Diez,[1,2] Elena Élez,[1,2] Jaume Capdevila,[1,2] Ana Oaknin,[1,2] Cristina Saura,[1,2] Teresa Macarulla,[1,2] Joan Carles Galceran,[1,2] Enriqueta Felip,[1,2] Rodrigo Dienstmann,[2] Philippe L. Bedard,[3] Paolo Nuciforo,[2] Joan Seoane,[2] Josep Tabernero,[1,2] Elena Garralda,[1,2,13] and Ana Vivancos[2,13,14,*]

SUMMARY

Background: Immunotherapy is effective, but current biomarkers for patient selection have proven modest sensitivity. Here, we developed VIGex, an optimized gene signature based on the expression level of 12 genes involved in immune response with RNA sequencing.

Methods: We implemented VIGex using the nCounter platform (Nanostring) on a large clinical cohort encompassing 909 tumor samples across 45 tumor types. VIGex was developed as a continuous variable, with cutoffs selected to detect three main categories (hot, intermediate-cold and cold) based on the different inflammatory status of the tumor microenvironment.

Findings: Hot tumors had the highest VIGex scores and exhibited an increased abundance of tumor-infiltrating lymphocytes as compared with the intermediate-cold and cold. VIGex scores varied depending on tumor origin and anatomic site of metastases, with liver metastases showing an immunosuppressive tumor microenvironment. The predictive power of VIGex-Hot was observed in a cohort of 98 refractory solid tumor from patients treated in early-phase immunotherapy trials and its clinical performance was confirmed through an extensive metanalysis across 13 clinically annotated gene expression datasets from 877 patients treated with immunotherapy agents. Last, we generated a pan-cancer biomarker platform that integrates VIGex categories with the expression levels of immunotherapy targets under development in early-phase clinical trials.

Conclusions: Our results support the clinical utility of VIGex as a tool to aid clinicians for patient selection and personalized immunotherapy interventions.

Funding: BBVA Foundation; 202–2021 Division of Medical Oncology and Hematology Fellowship award; Princess Margaret Cancer Center.

CONTEXT AND SIGNIFICANCE

There is an unmet need for predictive biomarkers that can identify patients more likely to benefit from immunotherapy. Researchers from the Vall d'Hebron University Hospital in Barcelona, Spain, have used real-world tumor samples from 45 different tumor types to develop VIGex, a gene expression signature that classifies tumors in three categories (hot, intermediate-cold, and cold). These three tumor groups are associated with different immunotherapy benefits. The authors validated their signature across laboratories and profiling platforms, showing that VIGex can be widely used and may help in personalizing novel immunotherapy combinations.

INTRODUCTION

The past decades have witnessed a rapid development of immunotherapy (IO) agents to treat cancer patients, and many of these have demonstrated profound anti-tumor activity across cancer types. Inhibitors of programmed death-1 (PD1)/programmed death-ligand-1 (PD-L1) immune checkpoints have been approved for multiple tumor types, either as monotherapy or in combination, and their administration is guided by measurement of PD-L1 levels by immunohistochemistry and quantification of the tumor mutational burden (TMB).[1–3] However, despite their unprecedented efficacy, patients with non-immunogenic histologies do not derive clinical benefit,[4] and for *a priori* immunogenic tumors current biomarkers fail to predict clinical responses in a large proportion of patients.[5] In an effort to address this clinical need, the drug development pipeline has experienced an unprecedented growth in the number of IO combinations, which has created the need for robust predictive pan-cancer IO biomarkers that guide patient selection in early-phase IO trials.[6] Investigation of the tumor microenvironment (TME) may unveil immunosuppressive pathways and strategies for increasing immunogenicity.[7]

Multi-gene signatures derived from representative sections of a tumor biopsy or surgical excision can provide a snapshot of the TME and the patient's immune response.[8] As an example, gene expression signatures have established clinical utility in the setting of risk stratification for early-stage breast cancer[9,10] and are used as pharmacodynamic endpoints to provide proof-of-target engagement for investigational drug treatments in early-phase IO trials.[11] A growing body of evidence suggests the potential role of the tumor transcriptome to predict outcomes in patients treated with IO.[12] An 18-gene signature of interferon gamma (IFNG) responsive genes that captures T cell inflamed states, was associated with IO benefit; however, this was developed based on the analysis of mainly immunogenic or "hot" tumors and its utility for predicting patient outcomes in a tumor-agnostic manner remains unclear.[12,13] Moreover, prior gene expression signatures have been developed solely in RNA sequencing (RNA-seq) or are based in an extensive number of genes.[14,15] Currently, RNA-seq protocols are not compatible with routine clinical workflows for a timely decision making.

To address these limitations, we developed a predictive, pan-cancer signature compatible with routine clinical testing, that captures the underlying immune contexture of tumors and can be used to prioritize IO combinations to treat patients in the context of early-phase clinical trials in oncology. The Vall d'Hebron Institute of Oncology (VHIO) gene expression signature (VIGex) is a 12-gene classifier selected from a list of 808 genes that form a cluster for adaptive immune response as per RNA-seq analysis of formalin-fixed paraffin-embedded (FFPE) tumor samples. The signature was implemented in the nCounter (Nanostring) platform and applied to a pan-cancer training cohort of 909 tumor samples from advanced solid tumor patients prospectively enrolled in the VHIO prescreening program[16] (see STAR methods). Three categories were identified (hot, intermediate-cold [I-Cold], and cold). VIGex categories were associated with IO benefit in patients treated with early-phase IO trials and in a metanalysis with publicly available datasets. Last, we integrated VIGex categories with the expression levels of IO targets under development in early-phase clinical trials generating a pan-cancer biomarker platform. Altogether, we present a highly scalable pan-cancer platform for patient selection for the next generation of IO trials.

RESULTS

Development of the VIGex signature

We first aimed to develop a tool to characterize the TME immunogenicity. We performed RNA-seq in 153 FFPE samples (see STAR methods) representing 23 tumor

[1]Department of Medical Oncology, Vall D'Hebron University Hospital, 08035 Barcelona, Spain

[2]Vall d'Hebron Institute of Oncology, 08035 Barcelona, Spain

[3]Division of Medical Oncology and Hematology, Department of Medicine, Princess Margaret Cancer Centre, University of Toronto, Toronto, ON M5G2C4, Canada

[4]Departamento de Medicina, Universidad Autónoma de Barcelona (UAB), 08035 Barcelona, Spain

[5]Institut du Cancer de Montréal, Centre de Recherche du Centre Hospitalier de l'Université de Montréal, Montréal, QC H2X0A9, Canada

[6]Faculty of Pharmacy, Université de Montréal, Montréal, QC H3T1J4, Canada

[7]Princess Margaret Cancer Centre, University Health Network, Toronto, ON M5G2C4, Canada

[8]Department of Medical Biophysics, University of Toronto, Toronto, ON M5G1L7, Canada

[9]Department of Computer Science, University of Toronto, Toronto, ON M5S2E4, Canada

[10]Ontario Institute for Cancer Research, Toronto, ON M5G0A3, Canada

[11]Vector Institute for Artificial Intelligence, Toronto, ON M5G1M1, Canada

[12]These authors contributed equally

[13]These authors contributed equally

[14]Lead contact

*Correspondence: avivancos@vhio.net

https://doi.org/10.1016/j.medj.2023.07.006

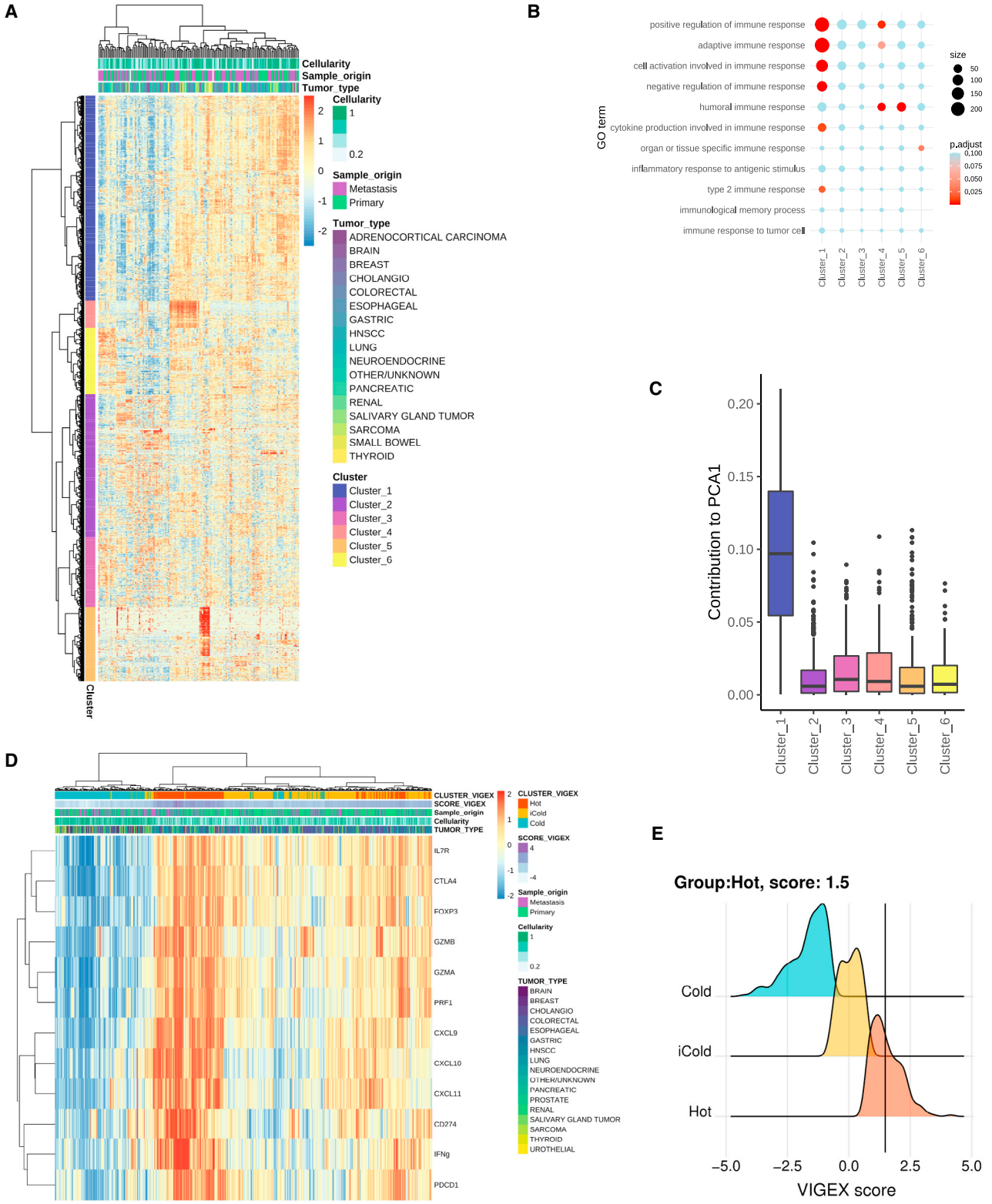

Figure 1. Development of the VIGex signature

(A) Heatmap showing gene expression of 2,323 genes including in the Gene Ontology (GO) term immune response (GO:0006955) within 153 samples analyzed with RNA sequencing (RNA-seq). The gene clusters identified with hierarchical clustering are highlighted.

Figure 1. *Continued*

(B) Dot plot showing an overrepresentation test for GO sub-terms in each cluster identified. The size of the dot is proportional to the number of genes included and the color represents the adjusted p value (Benjamini and Hochberg method).

(C) Boxplot showing gene contribution to principal-component analysis 1 (PCA1) in each cluster.

(D) Heatmap with 909 samples categorized with the VIGex signature in the nCounter platform (Nanostring) in the training dataset.

(E) Example of biopsy sample categorized by VIGex as hot with a continuous score.

types. A set of 2,323 genes included in the Gene Ontology (GO) term immune response (GO:0006955) were selected for further analysis. A hierarchical clustering classification was applied and six main clusters were identified (Figure 1A), each showing enrichment in particular GO sub-terms of the immune response (Figure 1B). Cluster 1 represented the most extensive percentage of explained variation in the first component of the principal-component analysis (PCA) (Figures 1C and S1A). Cluster 1 encompassed 808 genes related to adaptive immune response and regulation of immune responses reflective of IFNG-mediated inflammation. To develop a signature based on this cluster 1, we determined the minimum number of genes required to represent the average mean relative expression of the cluster (cluster 1 score). By testing combinations from 1 to 20 genes, correlations of the cluster 1 score with the Subset-cluster 1 scores were found to be highest using any subset of 12 or more genes of cluster 1 (median Pearson Correlation >0.78). Specifically, the addition of a more extensive number of genes did not relevantly increase the median Pearson Correlation (Figure S1B). The final 12-gene set encompassed genes involved in immune activation (*CXCL9*, *CXCL10*, *CXCL11*, *IFNG*, *PRF1*, *IL7R*, *GZMA,* and *GZMB*) and T cell exhaustion (*PDCD1*, *CTLA-4*, *CD274,* and *FOXP3*) markers with a role as IO response predictors or representing potential IO drug targets.[13,17–21] The VIGex 12-gene set score (VIGex score) was defined as the relative mean expression of these genes and was highly correlated with the score generated based on the 808 genes encompassing cluster 1 (Pearson correlation = 0.84; $p < 0.0001$) (see Figure S1B and STAR Methods). To evaluate the cross-platform analytical validation of the VIGex signature, we also tested the 12 selected genes in a subset of samples (n = 138) using the nCounter (Nanostring) platform (see STAR methods). Both individual gene expression levels and the VIGex score were highly correlated across RNA platforms (Nanostring vs. RNA-seq) (VIGex score Pearson correlation = 0.97; $p < 0.0001$) supporting signature development in both assays (Figures S1C–S1O).

We next sought to develop VIGex in the Nanostring platform using samples from 909 consecutive patients diagnosed with 45 different tumor types who were enrolled and underwent routine transcriptional profiling within the VHIO molecular prescreening program[16] (Figures 1D and 1E). Among these, a large number of samples comprised non-immunoreactive histologies (no Food and Drug Administration-approved IO agents) in our training dataset. This included pancreatic cancer (n = 67, 7%), brain tumors (n = 46, 5%), salivary gland tumors (n = 25, 3%), and other cold tumor histologies (n = 141, 16%) (Figure 2A). RNA isolated from FFPE tumor tissue samples was analyzed by nCounter (Nanostring) technology with a custom codeset including the VIGex 12-gene set. Hierarchical clustering and Partitioning Around Medoids (PAM) clustering of the transcriptomic data could further categorize samples into three main categories: hot, I-Cold, and cold based on decreasing expression levels of the 12-gene set. The existence of three categories was supported by the silhouette method.[22] This TME categorization was independent of clinical outcomes. VIGex score follows a normal distribution, and the cutoffs for defining hot (VIGex score >0.75), I-Cold (VIGex score between −0.75 and 0.75), and cold groups (VIGex score < −0.75), were selected based on the concordance with the groups obtained by two different clustering methods: hierarchical with three groups and PAM clustering (Figures S2A–S2C). Overall, these findings suggest the existence of three

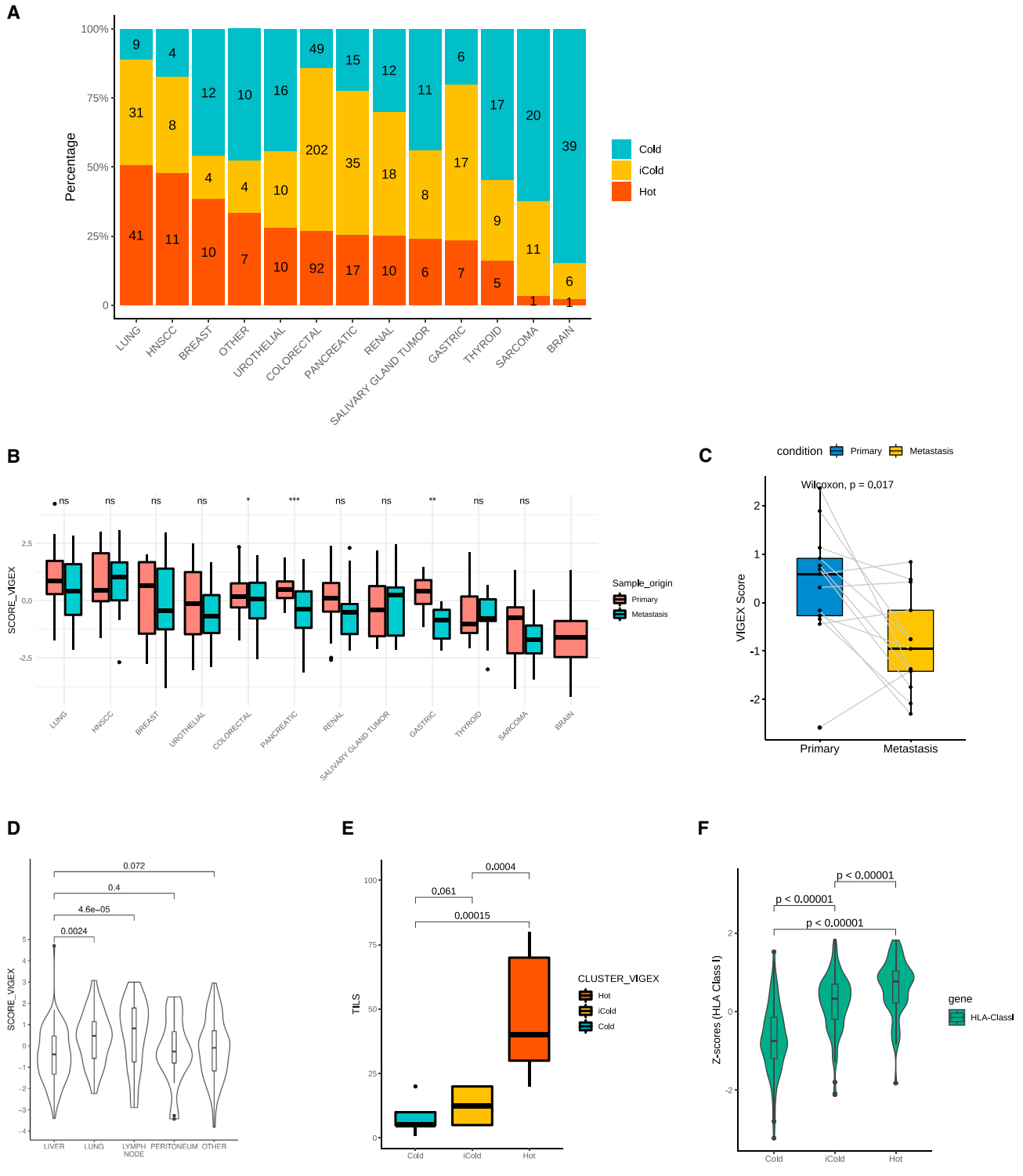

Figure 2. Analytical validation of VIGex

(A) Stacked bar plot showing the distribution of VIGex categories (hot, intermediate-cold, and cold) by tumor histology.

(B) Boxplot showing VIGex score in primary vs. metastatic samples stratified by tumor histology (t test). (ns represents a non-significant p value; *** represents a p value <0.001; ** represents a p value <0.01; * represents a p value <0.05.

(C) Boxplot displaying VIGex scores in matched primary-metastatic samples (N = 13 patients) (Wilcoxon test).

Figure 2. *Continued*

(D) Violin plot showing VIGex scores in metastatic samples located in liver vs. other anatomic sites of metastases (liver n = 130 samples; lung n = 27 samples; lymph node n = 42 samples; peritoneum n = 19 samples; other n = 99 samples) (Wilcoxon test).

(E) Boxplot displaying percentage of tumor-infiltrating lymphocytes (TILs) enrichment by tumor categories defined by VIGex (Wilcoxon test) (n = 33 samples).

(F) Violin plot showing *Z* scores of human leukocyte antigen (HLA) class I (HLA-A, HLA-B, and HLA-C) expression by tumor categories defined by VIGex (Wilcoxon test) (n = 324 samples).

categories (hot, I-Cold, and cold) with a decreasing inflammatory status characterizing the TME across tumor types. To confirm the interlaboratory consistency of the VIGex algorithm, 30 samples from patients enrolled in the VHIO prescreening program and previously analyzed with the nCounter (Nanostring) platform were sent to Princess Margaret Cancer Centre blinded for VIGex scoring and categorization. Total RNA-seq sample preparation and sequencing were performed at the Princess Margaret Cancer Centre and data files were sent back to VHIO for VIGex score and categories calculation (see STAR methods). VIGex continuous scores achieved very high correlation (Pearson correlation = 0.983; p value < 0.0001) (Figure S2D).

VIGex categorizes samples according to the immunogenicity of the tumor microenvironment

We first explored VIGex subgroup distribution by tumor type in the training dataset. Brain tumor samples were mostly categorized as I-Cold and cold. Non-small cell lung cancer (NSCLC) or head and neck squamous cell carcinoma (HNSCC) had the highest representation of the hot subgroup across tumor types. This suggests that the functional classification based on VIGex is consistent with *a priori* response rates observed in clinical trials testing anti-PD1/PD-L1 across tumor histologies and potential opportunities for IO treatments in less well characterized histologies such as salivary gland tumors[1,2,23,24] (Figure 2A).

Given emerging evidence suggesting that immune infiltrates and already approved biomarkers such as TMB or PD-L1 are heterogeneous not only between but also within tumors,[25] we reasoned that evaluation of VIGex signature could also be dependent on the tumor sample that was selected for analysis (metastasis vs. primary tumor). While some histologies showed equivalent VIGex scores in the primary tumor and metastatic samples (e.g., HNSCC, urothelial, breast, salivary gland tumors, and thyroid carcinoma), others displayed lower VIGex scores in the metastatic sites as compared with samples from the primary tumor (pancreatic, colorectal [CRC], gastric) (Figure 2B). In a subset of patients with paired samples from metastatic and primary tumor sites, the samples obtained from metastatic lesions displayed lower VIGex scores than those obtained from primary tumor tissue (p = 0.017) (Wilcoxon test) (Figure 2C). Emerging evidence suggests that the presence of liver metastases is associated with worse clinical outcomes in patients treated with IO.[26,27] Hence, we next explored whether the VIGex score may be also impacted by the anatomic site of metastasis analyzed. Among samples obtained from metastatic biopsies, liver and peritoneal metastatic disease were associated with numerically lower VIGex scores as compared with other anatomic biopsy sites, suggesting a more immunosuppressive TME across tumor types (Figure 2D). VIGex scores were also numerically lower in liver metastases for CRC (Figure S2E). To further evaluate the variability of VIGex accounting for biopsy quality metrics, we studied VIGex scores adjusted by tumor cellularity. Of note, no significant differences were observed in VIGex scores depending on tumor cellularity of tumor samples (Figures S2F–S2H).

The abundance of tumor-infiltrating lymphocytes (TILs) has been shown to be an independent prognostic factor in a variety of cancers. TILs density has been associated

A

Characteristic		No. (%)
Age	Median	59 (range 29-85)
Sex	Male	60 (61%)
	Female	38 (39%)
ECOG performance status	0	51 (52%)
	1	47 (48%)
Tumor type	Colorectal	37 (38%)
	HNSCC	11 (11%)
	Renal cell carcinoma	7 (7%)
	NSCLC	6 (6%)
	Other	37 (38%)
Number of prior lines	0	17 (17%)
	1	29 (29%)
	2	21 (21%)
	≥3	31 (32%)
Immunotherapy naïve	Yes	89 (91%)
	No	9 (9%)
Immunotherapy treatment	Anti-PD1	19 (19%)
	Anti-PD-L1	10 (10%)
	Anti-PD1/L1 combination	69 (70%)

B

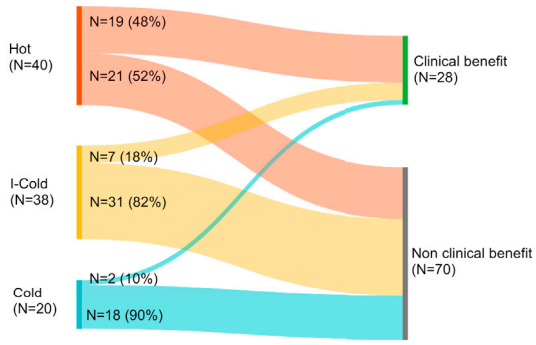

C

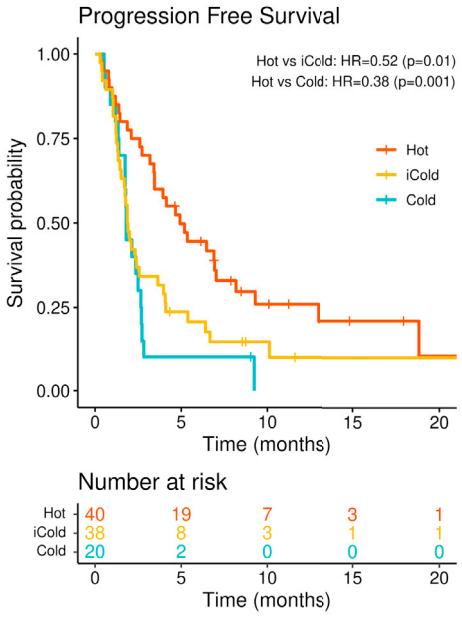

D

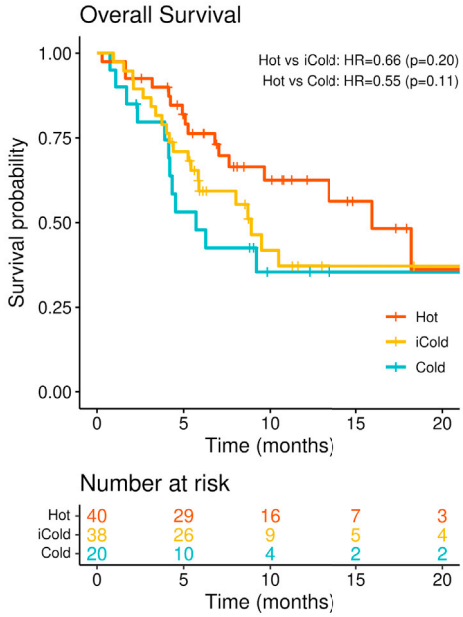

E

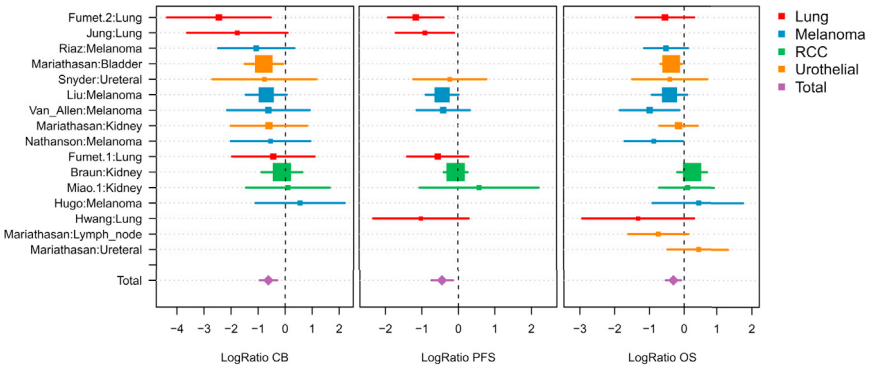

Figure 3. Clinical validation of VIGex

(A) Table summarizing baseline characteristics of the clinical validation cohort encompassing 98 patients treated with immunotherapy trials.

(B) Sankey diagram showing distribution of clinical benefit.

(C and D) Kaplan-Meier plot and Proportional Cox Hazard analysis of VIGex categories (hot, intermediate-cold [I-Cold], and cold) on progression-free survival (PFS) and overall survival (OS) in the clinical validation cohort (N = 98).

(E) Meta analysis of VIGex summarizing the performance of VIGex across publicly available datasets (Fumet.1,[34] Fumet.2,[34] Hugo,[14] Hwang,[35] Jung,[36] Riaz,[37] Braun,[38] Liu,[39] Mariathasan,[40] Miao.1,[41] Snyder,[42] Van_Allen[43] and Nathanson[44]). VIGex was associated with clinical benefit ($p < 0.001$), PFS ($p = 0.003$), and OS ($p = 0.006$). LogRatio CB is the natural logarithm of the odds ratio of the clinical benefit. LogRatio PFS and LogRatio OS is the natural logarithm of the hazard ratio of the progression-free survival and overall survival. RCC, renal cell carcinoma.

with better overall survival (OS) and improved IO outcomes.[28–30] We compared TILs enrichment in three different clusters as defined by the VIGex signature. A total of 33 tumor samples not included in the training dataset were interrogated for TILs density (see STAR methods). TILs density was significantly higher in the hot group as compared with the I-Cold ($p < 0.001$) or cold subtypes ($p < 0.001$) (Wilcoxon test) (Figure 2E). In all cells, the expression of major histocompatibility complex (MHC) I pathway components and surface MHC I levels are increased upon stimulation with interferons (IFNs), especially type 2 IFN (IFNG).[31] Across the training set of samples, a total of 324 samples were also tested for human leukocyte antigen (HLA) type 1 A, B, and C gene expression levels along the VIGex signature. We further interrogated whether differences in expression levels of HLA type 1 were observed between the VIGex groups. The cold category as defined by the VIGex signature showed lower expression of these genes when compared with the I-Cold or hot clusters ($p < 0.001$) and, likewise, the hot group had increased levels as compared with the I-Cold subgroup ($p < 0.001$) (Wilcoxon test), supporting that VIGex groups reflect IFNG signaling in tumors (Figure 2F).

VIGex identifies patients deriving clinical benefit in early-phase immuno-oncology trials

The predictive performance of VIGex was assessed in an independent cohort of 98 patients enrolled in early-phase IO trials at VHIO, treated with anti-PD1/PD-L1 monoclonal antibodies as monotherapy or in combination. VIGex was determined in baseline tumor samples obtained prior to IO treatment. The VIGex signature classified 40 (41%) patients as hot, 38 (39%) patients as I-Cold, and 20 (20%) patients as cold. Most frequent tumor histologies in this cohort included CRC (n = 37; 38%) with no differences in VIGex-Hot category depending on mismatch repair (MMR) status ($p = 0.4$) (Fisher's exact test), HNSCC (n = 11; 11%), and NSCLC (n = 6; 6%). Clinical benefit (CB) as defined by either complete/partial response or disease stabilization for $\geq$6 months was observed in 19 patients in the hot cluster (Clinical Benefit Rate [CBR] = 48%), seven patients in the I-Cold (CBR = 18%), and two patients in the cold cluster (CBR = 10%) ($p = 0.002$) (Fisher's exact test). Responses were observed in 13 patients in the hot cluster (objective response rate [ORR] = 33%), four in the I-Cold (ORR = 11%), and one patient in the cold cluster (ORR = 5%) ($p = 0.012$) (Fisher's exact test). The 12-month progression-free survival (PFS) rates were 26% for VIGex-Hot, 10% for I-Cold, and 0% for cold. Notably, the hot cluster was associated with longer PFS as compared with the I-Cold (HR = 0.52; 95% CI: 0.32–0.87; $p = 0.01$) or cold clusters (HR = 0.38; 95% CI: 0.21–0.68; $p = 0.001$). Importantly, differences in PFS were maintained when adjusted for number of prior treatment lines, Eastern Cooperative Oncology Group (ECOG) performance status, and type of IO regimen (monotherapy vs. combination) (HR = 0.43; 95% CI: 0.24–0.75; $p = 0.003$ for hot vs. I-Cold; HR = 0.28; 95% CI 0.15–0.57; $p < 0.001$ for hot vs. cold. Differences in OS within the three groups defined by VIGex did not reach statistical significance in this cohort (Figures 3A–3D). We next aimed to investigate the predictive power of VIGex in tumor-specific cohorts. VIGex categories were associated with PFS and OS in a dataset of HNSCC patients (GSE159067) treated with anti-PD1/L1

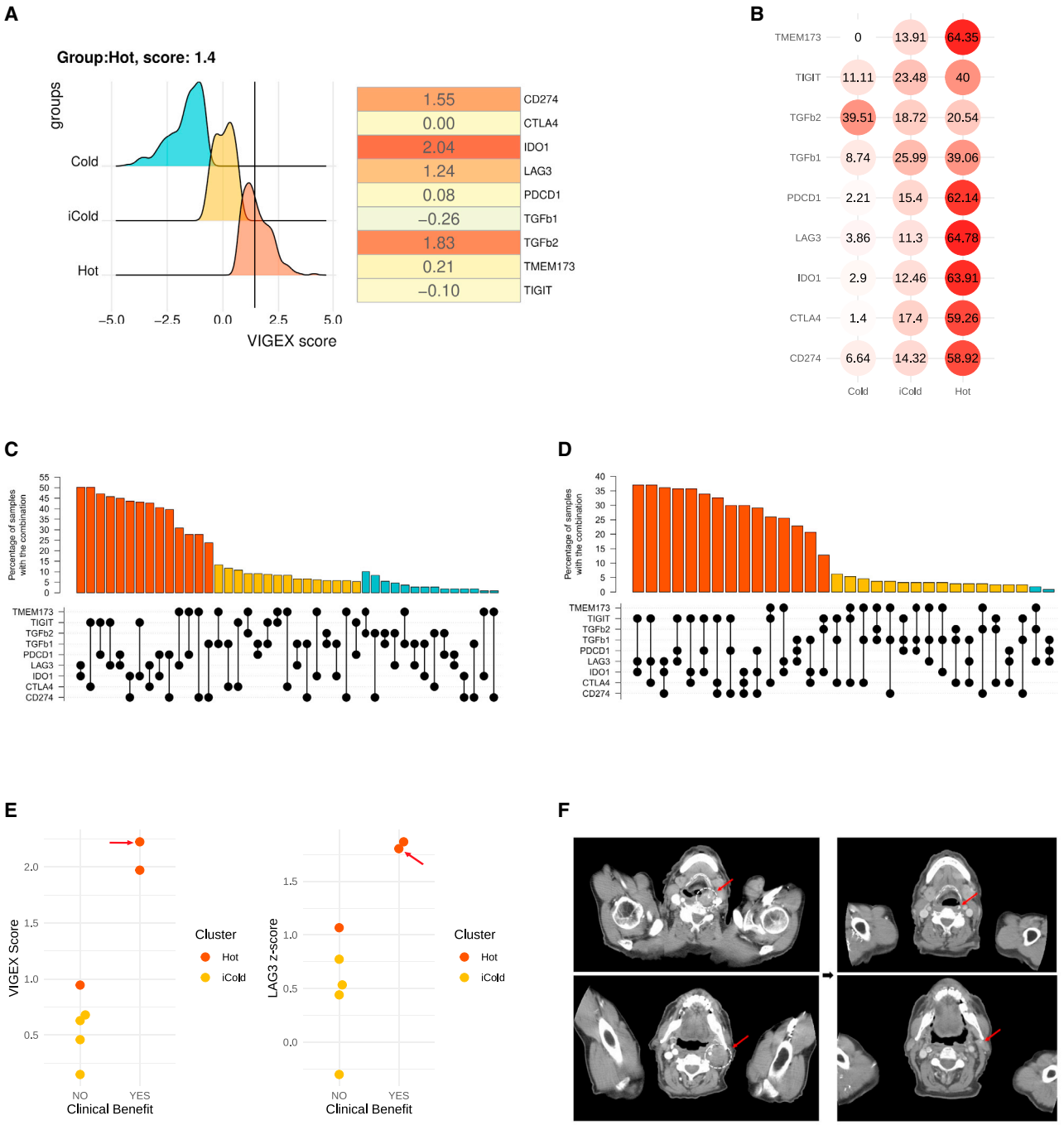

Figure 4. Association of VIGex categories with other immune markers involved in the cancer-immunity cycle under development in immuno-oncology trials

(A) Example of VIGex test output reported as a continuous score superimposed to the distribution of the scores of the samples included in the training dataset, with the *Z* score of selected immuno-oncology targets.

(B) Dot plot showing the percentage of overexpressed immuno-oncology targets in each of the VIGex categories in the training dataset. Overrepresentation cutoff is set at top 25% values for each gene. The intensity of the red color is proportional to the represented values.

(C and D) Bar plots summarizing the most recurrent co-expressed pairs (left) and triplets (right) of immuno-oncology targets within each VIGex subtype (samples considered for each group: hot [n = 227], intermediate-cold [I-Cold] [n = 241], and cold samples [n = 109]). Up to 15 co-expressed pairs and triplets of immuno-oncology targets are represented. For each pair/triplet, inclusive intersection is displayed. Each sample has at least overexpression in the selected immuno-oncology targets.

Figure 4. *Continued*

(E) Dot plot displaying VIGex score and *LAG3 Z* score across patients treated with anti-PD1/PD-L1 monoclonal antibodies and anti-LAG3 therapies, grouped by clinical benefit (N = 7). The red arrow identifies the case displayed in (F).

(F) Computed tomography (CT) scan evaluation at baseline and at the moment of best response of head and neck cancer patient classified as VIGex-Hot and *LAG3* overexpressed receiving a combination of anti-PD1 and anti-LAG3.

inhibitors ($p = 0.003$ and $p < 0.001$, respectively) (log rank test).[32] A trend toward significance was observed for the association of VIGex categories and PFS ($p = 0.17$) (log rank test) or OS ($p = 0.13$) (log rank test) in the GSE161537 dataset including NSCLC patients treated with IO with numerically higher 12-month PFS and OS rates for VIGex-Hot as compared with I-Cold or cold categories[32] (see Table S1). Moreover, VIGex categories were associated with PFS in patients with NSCLC treated with anti-PD1/L inhibitors alone or in combination with chemotherapy ($p = 0.011$) (log rank test) and OS in microsatellite instability high (MSI-H) CRC patients treated with anti-PD1/L1 inhibitors ($p = 0.032$) (log rank test). No significant differences were observed in OS in patients with microsatellite stable (MSS) CRC and pancreatic carcinoma from The Cancer Genome Atlas (TCGA),[33] suggesting IO specificity (Figures S2I–S2M and Table S1).

To further confirm the predictive power of the VIGex signature, we tested its performance in a metanalysis of publicly available gene expression datasets from patients treated with IO. The search strategy, consisting of a systematic review of the existent literature identified 13 available datasets investigating gene expression signatures and with IO annotated clinical data and outcome encompassing a total of 877 patients and six tumor types[14,34–44] (see STAR methods). VIGex was significantly associated with CB ($p < 0.001$), PFS ($p = 0.003$), and OS ($p = 0.006$) across available datasets (Figures 3E and S3A–S3C). Moreover, no significant differences were observed for VIGex, PD-L1, and TMB in performance for CB (Wilcoxon test) (Figure S3D). When further compared with already published gene expression signatures, the median area under the curve of VIGex for CB was 0.59 (interquartile range [IQR] = 0.57–0.62) across datasets with a numerically smaller IQR as compared with similar performing signatures, suggesting that the predictive power of VIGex is maintained across datasets and tumor types (Figure S3E). Last, numerical differences were observed in CB with the joint use of TMB and VIGex in different public datasets (Figure S3F) but no correlation was observed between these two biomarkers (Figures S3G–S3O and STAR methods).

A composite immune gene signature prioritizes immuno-oncology combinations in early-phase clinical trials

Individual gene-level information from specific immune markers may offer additive predictive power for selecting patients and matching them to particular IO agents or combinations. In addition to VIGex categories, we sought to explore other RNA-expression immune markers, in particular, individual gene expression levels using *Z* score units and their potential role to explore the TME using prior reported methodology.[45] The selection of genes may be customized. We aimed to explore additional genes with a role in the cancer-immunity cycle for which agents are currently under development in early-phase IO trials (*STING*, *TIGIT*, *IDO1*, *TGF-β1-2*, or *LAG3*).[46–51] Thus, VIGex test is reported as a combination of the VIGex score informing on the inflammatory status of the TME and *Z* scores for selected immune markers. As such, if a specific sample is informed as VIGex-Hot TME and *TGF-β* overexpression, a treatment based on anti-PD1/L1 monoclonal antibodies and *TGF-β* inhibitor could be proposed. An example of the output of VIGex to select the most appropriate IO combinations is included in Figure 4A. The distribution of gene expression profiles across individual immune targets was consistent with a normal distribution by the Q-Qplot test (Figures S4A–S4I) across the entire dataset (All Pearson correlations of expected vs. observed quantiles

were R > 0.98 and p values <0.0001). An overexpression cutoff was set at the top 25% values for each gene target. Noticeably, gene expression profiles of different immune markers were asymmetrically distributed across VIGex subtypes, with VIGex-Hot tumors more likely to express IO targets under development, such as *IDO1 or LAG3* (Figure 4B). Specific potential targets such as *TIGIT* and *TGF-β1* were overexpressed in I-Cold samples or *TGF-β2* in cold tumor samples suggesting therapeutic opportunities to enhance immunogenicity. Co-expression of doublets of IO markers within samples classified as hot, I-Cold, and cold categories by the VIGex signature were also investigated. Co-expression of *LAG3* and *IDO1*, *CTLA-4* and *TIGIT*, as well as *PDCD1* and *TIGIT*, were frequently observed in the VIGex-Hot subgroup, whereas immunosuppressive signals based on *TGF-β2* with a second immune marker were a frequent association in the cold samples by VIGex (Figure 4C). To further interrogate mechanism of resistance among I-Cold patients with CB and no-CB in our clinical validation dataset, *Z* scores from immune markers were compared. Notably, *TGF-β2* was significantly overexpressed in I-Cold patients with no-CB as compared with those with CB ($p = 0.049$) (Wilcoxon test). Recognizing the potential clinical value of triplet IO drug combinations to inhibit several immune pathways simultaneously, we aimed to explore the prevalence of co-expression of triplets of IO potential targets. Combinations of three targets were more frequently observed in tumors categorized as hot (e.g., 37% of hot samples showed co-expression of *LAG3*, *TIGIT,* and *IDO1*) (Figure 4D). Finally, we hypothesized that patients with increased RNA expression of the immune checkpoint *LAG3* gene may benefit from a combination of an anti-LAG3 monoclonal antibody with a PD1 immune checkpoint inhibitor. To provide a proof-of-concept of this hypothesis, we further interrogated the subgroup of patients treated with anti-PD1/PD-L1 plus anti-LAG3 in our clinical validation dataset. Among the 98 patients treated in early-phase IO trials at VHIO, seven patients were identified. Numerically higher VIGex and *LAG3* scores were observed in the two patients who achieved CB. Of note, one patient with recurrent HNSCC PD-L1 negative by immunohistochemistry (Dako 22C3 antibody) treated with anti-PD1 and anti-LAG3 achieved a complete response after progression following standard chemotherapy. The second patient with mucosal melanoma achieved a partial response with anti-PD1 and anti-LAG3 combination therapy after progression following anti-PD1, anti-CTLA4, and chemotherapy (Figures 4E and 4F). Overall, these findings support the implementation of immune gene-expression markers to interrogate the TME as a way to inform rational IO combination strategies.

DISCUSSION

The number of IO targets and IO drug combinations under development has rapidly expanded over the past decade. Despite this growth, the lack of robust IO biomarkers hinders the implementation of precision oncology in the early drug development setting with only a limited number of phase 1 IO trials including biomarker enrichment strategies to select the target population.[16] Recently, major advances in the field of cancer genomics have enabled the tumor-agnostic approval of pan-tumor genomic biomarkers such as TMB and deficient MMR or MSI (dMMR/MSI); however, only a few individuals will test positive for these biomarkers and an even more reduced subset of patients will benefit from IO interventions. RNA-based gene expression signatures are emerging as a potentially clinically useful approach to identify patients most likely to benefit from IO interventions. Here we present VIGex, a gene expression panel developed from RNA-seq and Nanostring profiles from 45 different tumor histologies. VIGex categories were significantly associated with TILs density and its performance tested across patients treated with investigational IO therapies including anti-PD1/PD-L1 monoclonal antibodies either as monotherapy or in combinations with other investigational IO therapies. We demonstrate that

VIGex identifies patients more likely to benefit from IO across tumor types and classes of IO therapies. Importantly, the performance of VIGex was maintained in a metanalysis across publicly available gene expression datasets from patients treated with IO and achieved similar performance to TMB for pan-cancer implementation.

Prior published signatures were developed by incorporating genes differentially expressed between responders and non-responders or have been trained using immunogenic tumors. VIGex, however, relies solely on RNA-seq and Nanostring profiles and has been developed from key genes involved in immune responses. The training set to define VIGex included advanced or metastatic tumor samples from the VHIO molecular prescreening program with a broad representation of histologies for which IO is not approved. Moreover, the ability to use stored FFPE tumor tissue for analysis on the Nanostring or RNA-seq platforms is well-suited to future clinical implementation. Importantly, a quick turnaround time of 2–3 weeks for the Nanostring results as previously reported,[16] will enable timely decision making for patient selection for the best IO therapies in the molecular tumor board. Similar to other established biomarkers, heterogeneity was observed across samples with those from liver metastatic sites displaying lower VIGex score as compared with other organs. Importantly, our findings are aligned with emerging data confirming the immunosuppressive role of liver metastases in disease evolution.[52] New technologies such as transcriptomic profiling of circulating tumor cells may be able to overcome this observed intrinsic heterogeneity.[53]

VIGex has value beyond its ability to predict the response to checkpoint blockade as it also provides a biological explanation of the intimate co-stimulatory and co-inhibitory factors present in the TME. It is noteworthy that different markers of the cancer-immunity cycle with available drugs in early-phase trials were differentially expressed across VIGex categories and across patients. This suggests that personalized IO interventions may be required to elicit responses in a broader population. The preliminary findings observed in our cohort where higher levels of *LAG3* gene expression were observed among the responsive patients treated with anti-PD1/PD-L1 and LAG3 inhibitors deserve further investigation. Moreover, the observation that the subset of patients with no-CB across I-Cold patients has overexpression of *TGF-β2* suggests the potential of *TGF-β* inhibitors-based IO combinations under development to revert immune-evasion.[48,54] The *Z* scores developed from gene expression levels based on novel IO targets could help to enrich patient selection for trials testing novel IO combination therapies with patients more likely to benefit. In the future, this could lead to the expansion of VIGex as a predictive marker for novel IO combinations as evidence evolves with the inclusion of novel IO investigational agents across phase 1 trials.

Limitations of the study

Our study has several limitations. First, the absence of information regarding other approved biomarkers such as PD-L1 expression or TMB in the cohort of patients treated with early-phase IO trials did not enable comparison of the performance of VIGex with these biomarkers. The numerically higher CB observed when using VIGex and TMB suggests that biomarker combinations will be required to improve predictions.[55] Moreover, the predictive accuracy of VIGex was investigated in a retrospective and heterogeneous cohort of patients treated with a variety of IO agents across early-phase IO trials. The fact that VIGex-Hot was associated with better IO outcomes in this heavily pretreated population supports the use of predictive biomarkers to improve patient selection after progression to standard of care regimens. Importantly, when included in a metanalysis from RNA-seq publicly available datasets, VIGex showed different performance across tumor types. This issue has been extensively reported across published gene expression signatures. Among the histologies included in our metanalysis, the best predictive power

was achieved in NSCLC and melanoma with worse performance in renal cell carcinoma. A potential explanation for this includes the co-existence of immunosuppressive pathways not captured by our signature in certain tumor types. In this regard, there is evidence that CD8 T cell infiltration may be related to a worse prognosis in renal cell carcinoma that is different from other tumor histologies.[38,56] In conclusion, our results confirm the analytical validation of the VIGex signature and its potential utility as a pan-cancer predictive biomarker to IO therapy. Further studies are needed to evaluate the correlation of VIGex with already approved biomarkers and to determine whether the co-expression of targets of IO combination therapies can be used to improve patient selection across novel IO combinations.

STAR★METHODS

Detailed methods are provided in the online version of this paper and include the following:

- KEY RESOURCES TABLE
- RESOURCE AVAILABILITY
  - Lead contact
  - Materials availability
  - Data and code availability
- EXPERIMENTAL MODELS AND STUDY PARTICIPANT DETAILS
- METHOD DETAILS
  - VHIO molecular profiling
  - VIGex inter-laboratory validation
  - Publicly available datasets of patients treated with immunotherapy in the metanalysis
  - VIGex and tumor mutational burden computation in the metanalysis
- QUANTIFICATION AND STATISTICAL ANALYSIS

SUPPLEMENTAL INFORMATION

Supplemental information can be found online at https://doi.org/10.1016/j.medj.2023.07.006.

ACKNOWLEDGMENTS

A.H.C. would like to acknowledge fellowship funding from the Spanish Society of Medical Oncology (SEOM), CRIS Contra el Cancer and Hold'em For Life Oncology Fellowship. This research has been funded by the Comprehensive Program of Cancer Immunotherapy & Immunology II (CAIMI-II) supported by the BBVA Foundation (grant 53/2021) and the 2020–2021 Division of Medical Oncology and Hematology (DMOH) Fellowship award at Princess Margaret Cancer Centre. VHIO would like to acknowledge the Cellex Foundation for providing research facilities and equipment and the CERCA Programme from the Generalitat de Catalunya for their support of this research. Authors from VHIO acknowledge the State Agency for Research (Agencia Estatal de Investigación) for providing financial support as a Center of Excellence Severo Ochoa (CEX2020-001024-S/AEI/10.13039/501100011033). A.V. was the recipient of a project award from the FAECC (AVP/18/AECC/3219) and received funding from the Advanced Molecular Diagnostic (DIAMAV) program from the FERO Foundation. Graphical abstract was created with BioRender.com. Diagram in Figure 3B was created with SankeyMATIC (sankeymatic.com).

AUTHOR CONTRIBUTIONS

Conceptualization, A.H.C., A.V., E.G., and P.L.B.; methodology, A.H.C., M.V.C., A.V., B.H.K., Y.B., F.A., and P.L.B. All of them had full access to the available data;

investigation, A.H.C., M.V.C., A.V., B.H.K., Y.B., F.A., and P.L.B.; writing – original draft, A.H.C.; writing – review & editing, A.H.C., M.V.C., A.V., B.H.K., Y.B., F.A., and P.L.B.; funding acquisition, A.H.C., A.V., E.G., and P.L.B.; project administration, A.H.C., E.G., A.V., and P.L.B; supervision, all the co-authors. All authors read and approved the final article and take responsibility for its content.

DECLARATION OF INTERESTS

A.H.C. reports travel and accommodation expenses from Merk Serono and Kyowa Kirin International. I.B. reports research funding for the present manuscript from Incyte, Merck Sharp & Dohme (MSD), Cellex Foundation, La Caixa Foundation, BBVA Foundation Comprehensive Program of Cancer Immunotherapy and Immunology (CAIMI) - (grant 89/2017). Other research funding as principal investigator: Astrazeneca, Bicycle therapeutics, Boehringer Ingellheim, Bristol Myers Squibb, Celgene, Dragonfly, GlaxoSmithkline, Gliknik, Immutep, ISA Pharmaceuticals, Janssen Oncology, Kura, Merck Serono, Nanobiotics, Novartis, Northern Biologics, Orion Pharma, Odonate Therapeutics, Regeneron, Pfizer, Sanofi, Pharmamar, Seattle Genetics, Shattuck Labs, and VCN Biosciences. Consulting fees: Achilles Therapeutics, Bristol Myers Squibb, Cancer Expert Now, eTheRNA immunotherapies, Merck Serono, Merck Sharp & Dohme (MSD), Rakuten pharma, Boehringer Ingellheim, and PCI biotech. Payment or honoraria: Bristol Myers Squibb, Merck Serono, Merck Sharp & Dohme (MSD). Support for attending meetings and/or travel: Merck Sharp &Dohme (MSD) and Merck Serono. Leadership or fiduciary role in other board, society, committee, or advocacy group, paid or unpaid: ESMO Head and Neck track, EORTC Head and Neck group and Cancer Core Europe Clinical Taskforce. Other financial or non-financial interests: Bristol Myers Squibb educational grant. J.S. reports Advisory Boards from: Surface Oncology and Tarus Therapeutics. Stocks/Shares, Personal: Surface Oncology. Research Grant, Institutional, Financial interest: Surface Oncology. B.H.K. is co-Founder of the MAQC (Massive Analysis and Quality Control) Society. SAB of: Consortium de recherche biopharmaceutique (CQDM), Quebec; Canada Break Through Cancer; Commonwealth Cancer Consortium, United States; Canadian Institute of Health Research – Institute of Genetics, Canada; IONIQ Sciences, US. Executive Committee of the Terry Fox Digital Health and Discovery Platform, Canada, and Board of Directors of AACR International – Canada, The American Association for Cancer Research, United States. Consultant for Code Ocean Inc, United States. T.J.P. reports Consulting or Advisory Role: Chrysallis Biomedical Advisors, Axiom Healthcare Strategies, and SAGA Diagnostics. Patents, Roaylties, other intellectual property: Hybrid-capture sequencing for determining immune cell clonality. Honoraria: Merck, AstraZeneca, Illumina, and PACT Pharma Research Funding: Roche. O.M. reports honoraria: Roche, Kyowa Kirin, Ferrer. Travel grant: Kyowa Kirin. C.V. reports financial interest as advisory board, personal: Bayer, Boehringer Ingelheim, GSK, Lilly, Mundipharma, PharmaMar. Invited speaker, personal: Roche. Local PI, Institutional, Financial interest, clinical trial: Adaptimmune, Ayala Therapeutics, Bayer (coordinating PI), Foghorn Therapeutics, Inhibrx, Karyopharm, and Lilly. Non-financial interest: GEIS-Spanish Sarcoma Group for Research, Member of Board of Directors. President since 2018. E.M. reports advisory boards from Amgen, Bristol-Myers Squibb, Merck Sharp & Dohme, Novartis, Pierre Fabre, Roche, Sanofi. Honoraria: Amgen, Bristol-Myers Squibb, Merck Sharp & Dohme, Novartis, Pierre Fabre, Roche. Clinical trial participation (principal investigator): Bristol-Myers Squibb, GlaxoSmithKline, Merck Sharp & Dohme, Novartis, Pierre Fabre, Roche. C.S reports financial interests as invited speaker from Astellas pharma, Bristol Myers Sqquib (Inst), Hoffmann-La Roche LTD, Ipsen, Pfizer S.L.U. Advisory board, personal: Astellas pharma, Bayer,

Bristol Myers Sqquib (Inst), Hoffmann-La Roche LTD, Ipsen, Merck Sharp Dohme, Pfizer S.L.U, Sanofi-Aventis. E.E. reports advisory boards from Amgen, Bayer, Hoffman LA-Roche, Merck Serono, MSD, Pierre Fabre, Sanofi, Servier. Invited Speaker, personal: Novartis, Organon. Funding, Institutional, Financial interest: Amgen Inc, Array Biopharma Inc, AstraZeneca Pharmaceuticals LP, BeiGene, Boehringer Ingelheim, Bristol-Myers Squibb International Corporation, Celgene International SARL, Debiopharm International SA, Genentech Inc, HalioDX SAS, Foffmann-La Roche Ltd, Hutchison MediPharma International, Janssen-Cilag SA, Medimmune, Menarini, Merck Health KGAA, Merck Sharp & Dohme de España SA, Merus NVS, Mirati, Novartis Farmaceútica SA, Pfizer, PharmaMar SA, Sanofi Aventis Recherche & Développement, Servier, and Taiho Pharma USA Inc. Non-Financial Interest: American Society of Clinical Oncology (ASCO), Other, Volunteer member of the ASCO Annual Meeting Scientific Program Committee: Developmental Therapeutics – Immunotherapy; European Society for Medical Oncology (ESMO), Other, Speaker of the ESMO Academy; Sociedad Española de Oncología Médica (SEOM), Other: Coordinator of the SEOM +MIR Section of Residents and Young Assistants. Other (travel accomodations, expenses): Amgen, Array BioPharma, Bristol-Myers Squibb, Merck Serono, Roche, Sanofi and Servier. J.C. reports personal conflicts of interest: Scientific consultancy role (Speaker and advisory roles) from Novartis, Pfizer, Ipsen, Exelixis, Bayer, Eisai, Advanced Accelerator Applications, Amgen, Sanofi, Lilly, Huchinson Pharma, ITM, Advanz, Merck Serono, Esteve, Roche. Research support: research grants from Novartis, Pfizer, Astrazeneca, Advanced Accelerator Applications, Eisai, Amgen, and Bayer. A.O. has served on advisory boards for Agenus, AstraZeceneca. Clovis Oncology, Inc., Corcept Therapeutics, Deciphera Pharmaceutical, Eisai Europe Limited, EMD Serono, Inc., F. Hoffmann-La Roche, GlaxoSmithKline, GOG, Immunogen, Medison Pharma, Merck Sharp & Dohme de España, Mersana Therapeutics, Novocure GmbH, Pharma Mar, prIME Oncology, ROCHE FARMA, Sattucklabs, Sutro Biopharma, Inc, and received support for travel or accommodation from Roche, AstraZeneca, PharmaMar and GSK. Clovis. C.S. has served as consultant, participated in advisory boards or received travel grants from: AstraZeneca, AX'Consulting, Byondis B.V, Daiichi Sankyo, Eisai, Exact Sciences, Exeter Pharma, F.Hoffmann-La Roche Ltd, ISSECAM, MediTech, Merck Sharp & Dohme, Novartis, Pfizer, Philips, Pierre Fabre, PintPharma, Puma Biotechnology, SeaGen, and Zymeworks. T.M. has received honoraria for consultancy from: Ability Pharmaceuticals, Amgen, AstraZeneca, Basilea Pharma, Baxter, BioLineRX Ltd, Celgene, Eisai, Ellipses, Esteve, Pharmaceuticals, Incyte, Ipsen Bioscience, Inc, Janssen, Lilly, MDS Medscape, Novocure, QED Therapeutics, Roche Farma, Sanofi-Aventis, Servier, and Zymeworks. Travel expenses from Servier, AstraZeneca, Sanofi, and Incyte. J.C. reports advisory boards from Astellas Pharma, AstraZeneca, Bayer, Johnson & Johnson, MSD Oncology, Novartis (AAA), Roche, Sanofi. Local PI, Institutional, No financial interest: Janssen-Cilag International NV. Lilly, S.A, Medimmune, Novartis Farmacéutica S.A, Sanofi-Aventis S.A. E.F. reports advisory boards from Amgen, Astra Zeneca, Bayer, Bristol-Myers Squibb, Daichi Sankyo, Eli Lilly, F. Hoffmann-La Roche, Glaxo Smith Kline, Janssen, Merck Sharp & Dohme, Merck Serono, Novartis, Peptomyc, Pfizer, Sanofi, Takeda. Invited speaker: Amgen, Astra Zeneca, Bristol-Myers Squibb, Eli Lilly, F. Hoffmann-La Roche, Janssen, Medscape, Merck Sharp & Dohme, Peervoice, Pfizer, Medical Trends, Merck Serono, Sanofi, Takeda, TouchOncology. Research funding: Merck Healthcare KGAa, Fundación Merck Salud. Independent member of the Board: Grífols. R.D. declares advisory role for Roche, Boehringer Ingelheim, received a speaker's fee from Roche, Boehringer Ingelheim, Ipsen, Amgen, Servier, Sanofi, Libbs, Merck Sharp & Dohme, Lilly and AstraZeneca and research grants from Merck and Pierre Fabre. P.B. is a local PI institutional: Amgen, AstraZeneca, Bicara, BMS, Genentech/Roche, Lilly, Merck,

Nektar Therapeutics, Novartis, Pfizer, Sanofi, SeaGen, and Zymeworks. Research grant, institutional: Pfizer. Funding, institutional: Servier. P.N. reports advisory board from Bayer, MSD Oncology. Invited speaker, personal: Novartis. Other, personal, consultant: Targos Molecular Pathology GmbH. J.S. reports membership on Board of Directors, personal: Northern Biologics Inc. Ownership interest, Personal, Co-Founder: Mosaic Biomedicals. Research Grant, Institutional, No financial interest: Astra Zeneca, Hoffmann-La Roche LTD, Isarna Therapeutics, Mosaic Biomedicals SL, Northern Biologics INC, Ridgeline Therapeutics and Roche Glycart AG. Non-financial interests: Asociación Española contra el cancer (Member of Board of Directors), European Association for Cancer Research (ECR) (Member of Board of Directors, Secretary General). J.T. reports personal financial interest in form of scientific consultancy role for Array Biopharma, AstraZeneca, Bayer, Boehringer Ingelheim, Chugai, Daiichi Sankyo, F. Hoffmann-La Roche Ltd, Genentech Inc, HalioDX SAS, Hutchison MediPharma International, Ikena Oncology, Inspirna Inc, IQVIA, Lilly, Menarini, Merck Serono, Merus, MSD, Mirati, Neophore, Novartis, Ona Therapeutics, Orion Biotechnology, Peptomyc, Pfizer, Pierre Fabre, Samsung Bioepis, Sanofi, Scandion Oncology, Scorpion Therapeutics, Seattle Genetics, Servier, Sotio Biotech, Taiho, Tessa Therapeutics, and TheraMyc. Stocks: Oniria Therapeutics and also educational collaboration with Imedex/HMP, Medscape Education, MJH Life Sciences, PeerView Institute for Medical Education and Physicians Education Resource (PER). E.G. reports consulting or advisory role: Roche, Ellipses pharma, Neomed Therapeutics, Janssen, Boehringer Ingelheim. Seattle Genetics. TFS. Alkermes. Thermo Fisher Scientific. Bristol-Myers Squibb. MabDiscovery. Anaveon. F-Star Therapeutics. Speakers Bureau MSD, Roche, Thermo Fisher Scientific and Lilly. Research funding (recipient institution): Novartis. Roche. Thermo Fisher Scientific, AstraZeneca/MEdImmune, Taiho Oncology, BeiGene. Other relationship (recipient institution): Affimed Gmbh, Amgen SA, Anaveon AG, AstraZeneca AB, Biontech Gmbh, Catalym Gmbh, CytomX Therapeutics. F. Hoffmann La Roche Ltd, F-Satar Beta Limited, Genentech Inc, Genmab B.v, Hutchison MEdipharma Limited, Imcheck Therapeutics, Immunoscore Ltd, Janssen-Cilag SA, Medimmune Llc, Merck kgga, Novartis Farmaceutica, S.a, peptomyc, Ribon Therapeutics, Roche Farma SA, Seattle Genetics Inc, Symphogen A/S, Taiho Pharma Usa Inc. A.V. reports advisory boards from Bayer, Bristol Meyers Squibb, Guardant Health, Incyte, Roche. Stocks or Shares: Reveal Genomics. Research grant, institutional, financial interest, preclinical research grant: Incyte and Roche.

Received: January 22, 2023
Revised: June 1, 2023
Accepted: July 14, 2023
Published: August 11, 2023

REFERENCES

1. Reck, M., Rodríguez-Abreu, D., Robinson, A.G., Hui, R., Csőszi, T., Fülöp, A., Gottfried, M., Peled, N., Tafreshi, A., Cuffe, S., et al. (2016). Pembrolizumab versus Chemotherapy for PD-L1–Positive Non–Small-Cell Lung Cancer. N. Engl. J. Med. *375*, 1823–1833.

2. Burtness, B., Harrington, K.J., Greil, R., Soulières, D., Tahara, M., de Castro, G., Psyrri, A., Basté, N., Neupane, P., Bratland, Å., et al. (2019). Pembrolizumab alone or with chemotherapy versus cetuximab with chemotherapy for recurrent or metastatic squamous cell carcinoma of the head and neck (KEYNOTE-048): a randomised, open-label, phase 3 study. Lancet *394*, 1915–1928.

3. Marabelle, A., Fakih, M., Lopez, J., Shah, M., Shapira-Frommer, R., Nakagawa, K., Chung, H.C., Kindler, H.L., Lopez-Martin, J.A., Miller, W.H., et al. (2020). Association of tumour mutational burden with outcomes in patients with advanced solid tumours treated with pembrolizumab: prospective biomarker analysis of the multicohort, open-label, phase 2 KEYNOTE-158 study. Lancet Oncol. *21*, 1353–1365.

4. Saavedra Santa Gadea, O., Hernando-Calvo, A., Berche, R., Vieito, M., Brana, I., Matos, I., Alonso, G., Galvao, V., Azaro, A., Oberoi, H.K., et al. (2021). Evaluating the role of immune-checkpoint inhibitor (ICI) combinations in patients (pts) with unselected "cold" tumors enrolled in early clinical trials (CT). J. Clin. Oncol. *39*, 2597.

5. McGrail, D.J., Pilié, P.G., Rashid, N.U., Voorwerk, L., Slagter, M., Kok, M., Jonasch, E., Khasraw, M., Heimberger, A.B., Lim, B., et al. (2021). High tumor mutation burden fails to predict immune checkpoint blockade response across all cancer types. Ann. Oncol. *32*, 661–672.

6. Upadhaya, S., Neftelino, S.T., Hodge, J.P., Oliva, C., Campbell, J.R., and Yu, J.X. (2021). Combinations take centre stage in PD1/PDL1 inhibitor clinical trials. Nat. Rev. Drug Discov. *20*, 168–169.

7. Ochoa de Olza, M., Navarro Rodrigo, B., Zimmermann, S., and Coukos, G. (2020). Turning up the heat on non-immunoreactive tumours: opportunities for clinical development. Lancet Oncol. *21*, e419–e430.

8. Ayers, M., Lunceford, J., Nebozhyn, M., Murphy, E., Loboda, A., Kaufman, D.R., Albright, A., Cheng, J.D., Kang, S.P., Shankaran, V., et al. (2017). IFN-γ-related mRNA profile predicts clinical response to PD-1 blockade. J. Clin. Invest. *127*, 2930–2940.

9. Sparano, J.A., van't Veer, L.J., Makower, D.F., Pritchard, K.I., Albain, K.S., Hayes, D.F., Geyer, C.E., Dees, E.C., Perez, E.A., Olson, J.A., et al. (2015). Prospective Validation of a 21-Gene Expression Assay in Breast Cancer. N. Engl. J. Med. Overseas. Ed. *373*, 2005–2014.

10. Sparano, J.A., Gray, R.J., Makower, D.F., Pritchard, K.I., Albain, K.S., Hayes, D.F., Geyer, C.E., Dees, E.C., Goetz, M.P., Olson, J.A., et al. (2018). Adjuvant Chemotherapy Guided by a 21-Gene Expression Assay in Breast Cancer. N. Engl. J. Med. *379*, 111–121.

11. Salawu, A., Hernando-Calvo, A., Chen, R.Y., Araujo, D. v, Oliva, M., Liu, Z.A., and Siu, L.L. (2022). Impact of pharmacodynamic biomarkers in immuno-oncology phase 1 clinical trials. Eur. J. Cancer *173*, 167–177.

12. Cristescu, R., Mogg, R., Ayers, M., Albright, A., Murphy, E., Yearley, J., Sher, X., Liu, X.Q., Lu, H., Nebozhyn, M., et al. (2018). Pan-tumor genomic biomarkers for PD-1 checkpoint blockade-based immunotherapy. Science *1979*, 362.

13. Murphy, E., Lunceford, J., Nebozhyn, M., Ayers, M., Loboda, A., Kaufman, D.R., Albright, A., Cheng, J.D., Kang, S.P., Shankaran, V., et al. (2017). IFN-γ–related mRNA profile predicts clinical response to PD-1 blockade Find the latest version : IFN-γ–related mRNA profile predicts clinical response to PD-1 blockade. J. Clin. Invest. *127*, 2930–2940.

14. Hugo, W., Zaretsky, J.M., Sun, L., Song, C., Moreno, B.H., Hu-Lieskovan, S., Berent-Maoz, B., Pang, J., Chmielowski, B., Cherry, G., et al. (2016). Genomic and Transcriptomic Features of Response to Anti-PD-1 Therapy in Metastatic Melanoma. Cell *165*, 35–44.

15. Auslander, N., Zhang, G., Lee, J.S., Frederick, D.T., Miao, B., Moll, T., Tian, T., Wei, Z., Madan, S., Sullivan, R.J., et al. (2018). Robust prediction of response to immune checkpoint blockade therapy in metastatic melanoma. Nat. Med. *24*, 1545–1549.

16. Dienstmann, R., Garralda, E., Aguilar, S., Sala, G., Viaplana, C., Ruiz-Pace, F., González-Zorelle, J., Grazia LoGiacco, D., Ogbah, Z., Ramos Masdeu, L., et al. (2020). Evolving Landscape of Molecular Prescreening Strategies for Oncology Early Clinical Trials. JCO Precis. Oncol. *4*, 505–513.

17. Kato, S., Okamura, R., Kumaki, Y., Ikeda, S., Nikanjam, M., Eskander, R., Goodman, A., Lee, S., Glenn, S.T., Dressman, D., et al. (2020). Expression of TIM3/VISTA checkpoints and the CD68 macrophage-associated marker correlates with anti-PD1/PDL1 resistance: implications of immunogram heterogeneity. OncoImmunology *9*, 1708065.

18. Litchfield, K., Reading, J.L., Puttick, C., Thakkar, K., Abbosh, C., Bentham, R., Watkins, T.B.K., Rosenthal, R., Biswas, D., Rowan, A., et al. (2021). Meta-analysis of tumor- and T cell-intrinsic mechanisms of sensitization to checkpoint inhibition. Cell *184*, 596–614.e14.

19. Pachynski, R.K., Morishima, C., Szmulewitz, R., Harshman, L., Appleman, L., Monk, P., Bitting, R.L., Kucuk, O., Millard, F., Seigne, J.D., et al. (2021). IL-7 expands lymphocyte populations and enhances immune responses to sipuleucel-T in patients with metastatic castration-resistant prostate cancer (mCRPC). J. Immunother. Cancer *9*, e002903.

20. Friedman, C., Ascierto, P., Davar, D., O'Hara, M., Shapira-Frommer, R., Dallos, M., Khemka, V., James, L., Fischer, B., Demes, S., et al. (2020). 393 First-in-human phase 1/2a study of the novel nonfucosylated anti–CTLA-4 monoclonal antibody BMS-986218 ± nivolumab in advanced solid tumors: initial phase 1 results. In Regular and young investigator award abstracts (BMJ Publishing Group Ltd)), pp. A239.1–A23239.

21. Revenko, A., Carnevalli, L.S., Sinclair, C., Johnson, B., Peter, A., Taylor, M., Hettrick, L., Chapman, M., Klein, S., Solanki, A., et al. (2022). Direct targeting of FOXP3 in Tregs with AZD8701, a novel antisense oligonucleotide to relieve immunosuppression in cancer. J. Immunother. Cancer *10*, e003892.

22. Shutaywi, M., and Kachouie, N.N. (2021). Silhouette Analysis for Performance Evaluation in Machine Learning with Applications to Clustering. Entropy *23*, 759.

23. Lombardi, G., Barresi, V., Indraccolo, S., Simbolo, M., Fassan, M., Mandruzzato, S., Simonelli, M., Caccese, M., Pizzi, M., Fassina, A., et al. (2020). Pembrolizumab Activity in Recurrent High-Grade Gliomas with Partial or Complete Loss of Mismatch Repair Protein Expression: A Monocentric, Observational and Prospective Pilot Study. Cancers *12*, 2283.

24. Even, C., Delord, J.-P., Price, K.A., Nakagawa, K., Oh, D.-Y., Burge, M., Chung, H.C., Doi, T., Fakih, M., Takahashi, S., et al. (2022). Evaluation of pembrolizumab monotherapy in patients with previously treated advanced salivary gland carcinoma in the phase 2 KEYNOTE-158 study. Eur. J. Cancer *171*, 259–268.

25. Rosenthal, R., Cadieux, E.L., Salgado, R., Bakir, M.A., Moore, D.A., Hiley, C.T., Lund, T., Tanić, M., Reading, J.L., Joshi, K., et al. (2019). Neoantigen-directed immune escape in lung cancer evolution. Nature *567*, 479–485.

26. Emens, L.A., Cruz, C., Eder, J.P., Braiteh, F., Chung, C., Tolaney, S.M., Kuter, I., Nanda, R., Cassier, P.A., Delord, J.-P., et al. (2019). Long-term Clinical Outcomes and Biomarker Analyses of Atezolizumab Therapy for Patients With Metastatic Triple-Negative Breast Cancer. JAMA Oncol. *5*, 74–82.

27. Bilen, M.A., Shabto, J.M., Martini, D.J., Liu, Y., Lewis, C., Collins, H., Akce, M., Kissick, H., Carthon, B.C., Shaib, W.L., et al. (2019). Sites of metastasis and association with clinical outcome in advanced stage cancer patients treated with immunotherapy. BMC Cancer *19*, 857.

28. Yasunaga, M., Tabira, Y., Nakano, K., Iida, S., Ichimaru, N., Nagamoto, N., and Sakaguchi, T. (2000). Accelerated growth signals and low tumor-infiltrating lymphocyte levels predict poor outcome in T4 esophageal squamous cell carcinoma. Ann. Thorac. Surg. *70*, 1634–1640.

29. Fu, Q., Chen, N., Ge, C., Li, R., Li, Z., Zeng, B., Li, C., Wang, Y., Xue, Y., Song, X., et al. (2019). Prognostic value of tumor-infiltrating lymphocytes in melanoma: a systematic review and meta-analysis. OncoImmunology *8*, 1593806.

30. Pagès, F., Mlecnik, B., Marliot, F., Bindea, G., Ou, F.-S., Bifulco, C., Lugli, A., Zlobec, I., Rau, T.T., Berger, M.D., et al. (2018). International validation of the consensus Immunoscore for the classification of colon cancer: a prognostic and accuracy study. Lancet *391*, 2128–2139.

31. Zhou, F. (2009). Molecular Mechanisms of IFN-γ to Up-Regulate MHC Class I Antigen Processing and Presentation. Int. Rev. Immunol. *28*, 239–260.

32. Foy, J.-P., Karabajakian, A., Ortiz-Cuaran, S., Boussageon, M., Michon, L., Bouaoud, J., Fekiri, D., Robert, M., Baffert, K.-A., Hervé, G., et al. (2022). Datasets for gene expression profiles of head and neck squamous cell carcinoma and lung cancer treated or not by PD1/PD-L1 inhibitors. Data Brief *44*, 108556.

33. Goldman, M.J., Craft, B., Hastie, M., Repečka, K., McDade, F., Kamath, A., Banerjee, A., Luo, Y., Rogers, D., Brooks, A.N., et al. (2020). Visualizing and interpreting cancer genomics data via the Xena platform. Nat. Biotechnol. *38*, 675–678.

34. Fumet, J.D., Richard, C., Ledys, F., Klopfenstein, Q., Joubert, P., Routy, B., Truntzer, C., Gagné, A., Hamel, M.A., Guimaraes, C.F., et al. (2018). Prognostic and predictive role of CD8 and PD-L1 determination in lung tumor tissue of patients under anti-PD-1 therapy. Br. J. Cancer *119*, 950–960.

35. Hwang, S., Kwon, A.Y., Jeong, J.Y., Kim, S., Kang, H., Park, J., Kim, J.H., Han, O.J., Lim, S.M., and An, H.J. (2020). Immune gene signatures for predicting durable clinical benefit of anti-PD-1 immunotherapy in patients with non-small cell lung cancer. Sci. Rep. *10*, 643–710.

36. Jung, H., Kim, H.S., Kim, J.Y., Sun, J.-M., Ahn, J.S., Ahn, M.-J., Park, K., Esteller, M., Lee, S.-H., and Choi, J.K. (2019). DNA methylation loss promotes immune evasion of tumours with high mutation and copy number load. Nat. Commun. *10*, 4278.

37. Riaz, N., Havel, J.J., Makarov, V., Desrichard, A., Urba, W.J., Sims, J.S., Hodi, F.S., Martín-Algarra, S., Mandal, R., Sharfman, W.H., et al. (2017). Tumor and Microenvironment Evolution during Immunotherapy with Nivolumab. Cell *171*, 934–949.e16.

38. Braun, D.A., Hou, Y., Bakouny, Z., Ficial, M., Sant' Angelo, M., Forman, J., Ross-Macdonald, P., Berger, A.C., Jegede, O.A., Elagina, L., et al. (2020). Interplay of somatic alterations and immune infiltration modulates response to

PD-1 blockade in advanced clear cell renal cell carcinoma. Nat. Med. *26*, 909–918.

39. Liu, D., Schilling, B., Liu, D., Sucker, A., Livingstone, E., Jerby-Arnon, L., Zimmer, L., Gutzmer, R., Satzger, I., Loquai, C., et al. (2019). Integrative molecular and clinical modeling of clinical outcomes to PD1 blockade in patients with metastatic melanoma. Nat. Med. *25*, 1916–1927.

40. Mariathasan, S., Turley, S.J., Nickles, D., Castiglioni, A., Yuen, K., Wang, Y., Kadel, E.E., Koeppen, H., Astarita, J.L., Cubas, R., et al. (2018). TGFβ attenuates tumour response to PD-L1 blockade by contributing to exclusion of T cells. Nature *554*, 544–548.

41. Miao, D., Miao, D., Margolis, C.A., Gao, W., Voss, M.H., Li, W., Martini, D.J., Norton, C., Bossé, D., Wankowicz, S.M., et al. (2018). Genomic correlates of response to immune checkpoint therapies in clear cell renal cell carcinoma. Science *5951*, 1–11.

42. Snyder, A., Nathanson, T., Funt, S.A., Ahuja, A., Buros Novik, J., Hellmann, M.D., Chang, E., Aksoy, B.A., Al-Ahmadie, H., Yusko, E., et al. (2017). Contribution of systemic and somatic factors to clinical response and resistance to PD-L1 blockade in urothelial cancer: An exploratory multi-omic analysis. PLoS Med. *14*, e1002309.

43. Van Allen, E.M., Miao, D., Schilling, B., Shukla, S.A., Blank, C., Zimmer, L., Sucker, A., Hillen, U., Foppen, M.H.G., Goldinger, S.M., et al. (2015). Genomic correlates of response to CTLA-4 blockade in metastatic melanoma. Science *350*, 207–211.

44. Nathanson, T., Ahuja, A., Rubinsteyn, A., Aksoy, B.A., Hellmann, M.D., Miao, D., Van Allen, E., Merghoub, T., Wolchok, J.D., Snyder, A., and Hammerbacher, J. (2017). Somatic Mutations and Neoepitope Homology in Melanomas Treated with CTLA-4 Blockade. Cancer Immunol. Res. *5*, 84–91.

45. Sánchez-Guixé, M., Hierro, C., Jiménez, J., Viaplana, C., Villacampa, G., Monelli, E., Brasó-Maristany, F., Ogbah, Z., Parés, M., Guzmán, M., et al. (2022). High FGFR1-4 mRNA Expression Levels Correlate with Response to Selective FGFR Inhibitors in Breast Cancer. Clin. Cancer Res. *28*, 137–149.

46. Freeman, Z.T., Nirschl, T.R., Hovelson, D.H., Johnston, R.J., Engelhardt, J.J., Selby, M.J., Kochel, C.M., Lan, R.Y., Zhai, J., Ghasemzadeh, A., et al. (2020). A conserved intratumoral regulatory T cell signature identifies 4-1BB as a pan-cancer target. J. Clin. Invest. *130*, 1405–1416.

47. Chin, E.N., Yu, C., Vartabedian, V.F., Jia, Y., Kumar, M., Gamo, A.M., Vernier, W., Ali, S.H., Kissai, M., Lazar, D.C., et al. (2020). Antitumor activity of a systemic STING-activating non-nucleotide cGAMP mimetic. Science *369*, 993–999.

48. Bedard, P.L., Hernando-Calvo, A., Carvajal, R.D., Morris, V.K., Paik, P.K., Zandberg, D.P., Kaczmar, J.M., Niculescu, L., Bohr, D., Reiners, R., et al. (2022). A phase 1 trial of the bifunctional EGFR/TGFβ fusion protein BCA101 alone and in combination with pembrolizumab in patients with advanced solid tumors. J. Clin. Oncol. *40*, 2513.

49. Tawbi, H.A., Schadendorf, D., Lipson, E.J., Ascierto, P.A., Matamala, L., Castillo Gutiérrez, E., Rutkowski, P., Gogas, H.J., Lao, C.D., de Menezes, J.J., et al. (2022). Relatlimab and Nivolumab versus Nivolumab in Untreated Advanced Melanoma. N. Engl. J. Med. *386*, 24–34.

50. Tang, K., Wu, Y.-H., Song, Y., and Yu, B. (2021). Indoleamine 2,3-dioxygenase 1 (IDO1) inhibitors in clinical trials for cancer immunotherapy. J. Hematol. Oncol. *14*, 68.

51. Chauvin, J.-M., and Zarour, H.M. (2020). TIGIT in cancer immunotherapy. J. Immunother. Cancer *8*, e000957.

52. Yu, J., Green, M.D., Li, S., Sun, Y., Journey, S.N., Choi, J.E., Rizvi, S.M., Qin, A., Waninger, J.J., Lang, X., et al. (2021). Liver metastasis restrains immunotherapy efficacy via macrophage-mediated T cell elimination. Nat. Med. *27*, 152–164.

53. Negishi, R., Yamakawa, H., Kobayashi, T., Horikawa, M., Shimoyama, T., Koizumi, F., Sawada, T., Oboki, K., Omuro, Y., Funasaka, C., et al. (2022). Transcriptomic profiling of single circulating tumor cells provides insight into human metastatic gastric cancer. Commun. Biol. *5*, 20.

54. Guo, Y., Liu, B., Lv, D., Cheng, Y., Zhou, T., Zhong, Y., Hu, C., Chen, G., Wu, X., Yin, Y., et al. (2022). Phase I/IIa study of PM8001, a bifunctional fusion protein targeting PD-L1 and TGF-β, in patients with advanced tumors. J. Clin. Oncol. *40*, 2512.

55. Pender, A., Titmuss, E., Pleasance, E.D., Fan, K.Y., Pearson, H., Brown, S.D., Grisdale, C.J., Topham, J.T., Shen, Y., Bonakdar, M., et al. (2021). Genome and Transcriptome Biomarkers of Response to Immune Checkpoint Inhibitors in Advanced Solid Tumors. Clin. Cancer Res. *27*, 202–212.

56. Braun, D.A., Bakouny, Z., Hirsch, L., Flippot, R., van Allen, E.M., Wu, C.J., and Choueiri, T.K. (2021). Beyond conventional immune-checkpoint inhibition - novel immunotherapies for renal cell carcinoma. Nat. Rev. Clin. Oncol. *18*, 199–214.

57. Nuciforo, P., Pascual, T., Cortés, J., Llombart-Cussac, A., Fasani, R., Paré, L., Oliveira, M., Galvan, P., Martínez, N., Bermejo, B., et al. (2018). A predictive model of pathologic response based on tumor cellularity and tumor-infiltrating lymphocytes (CelTIL) in HER2-positive breast cancer treated with chemo-free dual HER2 blockade. Ann. Oncol. *29*, 170–177.

58. Hendry, S., Salgado, R., Gevaert, T., Russell, P.A., John, T., Thapa, B., Christie, M., van de Vijver, K., Estrada, M. v, Gonzalez-Ericsson, P.I., et al. (2017). Assessing Tumor-infiltrating Lymphocytes in Solid Tumors: A Practical Review for Pathologists and Proposal for a Standardized Method From the International Immunooncology Biomarkers Working Group: Part 1: Assessing the Host Immune Response, TILs in Invasive Breast Carcinoma and Ductal Carcinoma In Situ, Metastatic Tumor Deposits and Areas for Further Research. Adv. Anat. Pathol. *24*, 235–251.

59. Hendry, S., Salgado, R., Gevaert, T., Russell, P.A., John, T., Thapa, B., Christie, M., van de Vijver, K., Estrada, M. v, Gonzalez-Ericsson, P.I., et al. (2017). Assessing Tumor-Infiltrating Lymphocytes in Solid Tumors: A Practical Review for Pathologists and Proposal for a Standardized Method from the International Immuno-Oncology Biomarkers Working Group: Part 2: TILs in Melanoma, Gastrointestinal Tract Carcinomas, Non-Small Cell Lung Carcinoma and Mesothelioma, Endometrial and Ovarian Carcinomas, Squamous Cell Carcinoma of the Head and Neck, Genitourinary Carcinomas, and Primary Brain Tumors. Adv. Anat. Pathol. *24*, 311–335.

60. Dobin, A., Davis, C.A., Schlesinger, F., Drenkow, J., Zaleski, C., Jha, S., Batut, P., Chaisson, M., and Gingeras, T.R. (2013). STAR: ultrafast universal RNA-seq aligner. Bioinformatics *29*, 15–21.

61. Li, B., and Dewey, C.N. (2011). RSEM: accurate transcript quantification from RNA-Seq data with or without a reference genome. BMC Bioinf. *12*, 323.

62. Bareche, Y., Kelly, D., Abbas-Aghababazadeh, F., Nakano, M., Esfahani, P.N., Tkachuk, D., Mohammad, H., Samstein, R., Lee, C.-H., Morris, L.G.T., et al. (2022). Leveraging Big Data of Immune Checkpoint Blockade Response Identifies Novel Potential Targets. Ann. Oncol. *33*, 1304–1317.

63. Patro, R., Duggal, G., Love, M.I., Irizarry, R.A., and Kingsford, C. (2017). Salmon provides fast and bias-aware quantification of transcript expression. Nat. Methods *14*, 417–419.

64. Hänzelmann, S., Castelo, R., and Guinney, J. (2013). GSVA: gene set variation analysis for microarray and RNA-seq data. BMC Bioinf. *14*, 7.

65. Therneau, T. (2022). A Package for Survival Analysis in R. R Package Version 3.4-0. https://CRAN.R-project.org/package=survival.

66. Borenstein, M., and Higgins, J.P.T. (2013). Meta-Analysis and Subgroups. Prev. Sci. *14*, 134–143.

67. Higgins, J.P.T., Thompson, S.G., Deeks, J.J., and Altman, D.G. (2003). Measuring inconsistency in meta-analyses. BMJ *327*, 557–560.

68. Lin, L., Chu, H., and Hodges, J.S. (2017). Analysis : Reducing the Impact of Outlying Studies. Biometrics *73*, 156–166.

69. Whitehead, A., and Whitehead, J. (1991). A general parametric approach to the meta-analysis of randomized clinical trials. Stat. Med. *10*, 1665–1677.

STAR★METHODS

KEY RESOURCES TABLE

REAGENT or RESOURCE	SOURCE	IDENTIFIER
Deposited data		
Clinical dataset VHIO (N = 98)	VHIO prescreening program	http://github.com/mariavica/VIGex
GSE159067	Foy et al.[32]	http://github.com/mariavica/VIGex
GSE161537	Foy et al.[32]	http://github.com/mariavica/VIGex
NSCLC VHIO	VHIO prescreening program	http://github.com/mariavica/VIGex
MSI-H CRC VHIO	VHIO prescreening program	http://github.com/mariavica/VIGex
TCGA MSS CRC	TCGA[33]	http://github.com/mariavica/VIGex
TCGA Pancreatic cancer	TCGA[33]	http://github.com/mariavica/VIGex
Fumet.1	Fumet et al.[34]	https://codeocean.com/capsule/6760186/tree and https://predictio.ca.
Fumet.2	Fumet et al.[34]	https://codeocean.com/capsule/6760186/tree and https://predictio.ca.
Hugo	Hugo et al.[14]	https://codeocean.com/capsule/6760186/tree and https://predictio.ca.
Hwang	Hwang et al.[35]	https://codeocean.com/capsule/6760186/tree and https://predictio.ca.
Jung	Jung et al.[36]	https://codeocean.com/capsule/6760186/tree and https://predictio.ca.
Riaz	Riaz et al.[37]	https://codeocean.com/capsule/6760186/tree and https://predictio.ca.
Braun	Braun et al.[38]	https://codeocean.com/capsule/6760186/tree and https://predictio.ca.
Liu	Liu et al.[39]	https://codeocean.com/capsule/6760186/tree and https://predictio.ca.
Mariathasan	Mariathasan et al.[40]	https://codeocean.com/capsule/6760186/tree and https://predictio.ca.
Miao.1	Miao et al.[41]	https://codeocean.com/capsule/6760186/tree and https://predictio.ca.
Snyder	Snyder et al.[42]	https://codeocean.com/capsule/6760186/tree and https://predictio.ca.
Van_Allen	Van Allen et al.[43]	https://codeocean.com/capsule/6760186/tree and https://predictio.ca.
Nathanson	Nathason et al.[44]	https://codeocean.com/capsule/6760186/tree and https://predictio.ca.
Software and algorithms		
R software	https://www.r-project.org/	v3.6.3

RESOURCE AVAILABILITY

Lead contact

Further information and requests for resources will be fulfilled by the lead contact, Ana Vivancos (avivancos@vhio.net).

Materials availability

This study did not generate new unique reagents.

Data and code availability

- Clinical and RNA data are available in http://github.com/mariavica/VIGex and included as supplementary material.
- VIGex validation in the metanalysis of publicly available datasets, tested signatures, and code are available at https://codeocean.com/capsule/6760186/tree and in the following web-application https://predictio.ca.
- Any additional information required to reanalyze the data reported in this paper is available from the lead contact upon request.

EXPERIMENTAL MODELS AND STUDY PARTICIPANT DETAILS

Patients enrolled in the VHIO prescreening program had their tumors profiled by means of RNA-seq or Nanostring technology. Eligible patients were ≥18 years old with diagnosis of advanced or metastatic solid malignancies. Patients require an ECOG ≤1 performance status and available archival or fresh tumor tissue. A tumor tissue obtained from the most recent tissue collection procedure at the time of enrollment was used for profiling. A section of the FFPE tissue was examined with hematoxylin and eosin staining to confirm presence of invasive tumor cells and determine the tumor area. Participants information on sex was self-reported. Information on gender, socioeconomic status was not collected for VHIO clinical datasets.

METHOD DETAILS

VHIO molecular profiling

RNA-Seq gene expression analysis were conducted through Capture RNA-Seq of 153 FFPE tissue samples using TruSeq RNA Library Prep for Enrichment from Illumina following manufactures guides. The 153 FFPE samples included 146 archival and 7 fresh biopsies. Eighty samples were surgical resections, 50 core biopsies, 13 endoscopic biopsies, 7 incisional biopsies, 2 fine needle aspirations and 1 punch biopsy. The overall percentage of failure is 7.8% for RNA-seq profiling. Briefly, after conversion of RNA (50–200 μg) to cDNA and double stranded cDNA, sequencing adapters (TruSeq RNA Single Indexes Set A and Set B, Illumina) were ligated and PCR amplified with 12–15 cycles, depending on RNA input. The coding regions (CDS) of the transcriptome were doubly captured from amplified libraries using sequence-specific probes (Exome Panel, Illumina) to create the final library (TruSeq RNA Enrichment). Paired-end 2X75-bp sequencing were performed in the Illumina NextSeq 550 with an average of 70 millions of reads. Sequencing reads were quality controlled with FastQC 0.11.9. Low quality and contaminant reads were trimmed using Trimmomatic 0.39. Good quality reads were mapped to the human reference (hg38) with STAR 2.7.4a. The mapping parameters were based upon the best practices for STAR, adjusting the library type to strand-specific-reverse. To examine sequencing alignment data and provide statistical analyses Qualimap v2.2.1 were used. Counts were obtained using HTSeq count 0.13.5. DESeq2 R/Bioconductor package (1.36.0) was used to perform the counts normalization. Hierarchical clustering was done with euclidean distance and "ward.D2" method.

For Nanostring profiling, 250 ng of total RNA, quantified using the NanoDrop 2000 (Thermo Scientific), was directly hybridized (at 65°C for 18 h) with a mixture of biotinylated capture probes and fluorescently labeled reporter probes complementary to target sequences. After solution-phase hybridization between target RNA and reporter-capture probe pairs, excess probes were washed away using a two steps magnetic bead-based purification on the nCounter Prep Station. Finally, the RNA/Probe complexes were aligned and immobilized in the cartridge for data collection. The cartridge was then transferred to the nCounter Digital Analyzer for image acquisition and counts collection. Gene expression values were first normalized to the positive controls and then normalized to the geometric mean expression of the included 17 housekeeping genes and a total of 19 probes (*ACTB*, *ALAS1*, *CHMP2A* exon 1, *CHMP2A* exon 3, *CLTC*, *EMC7* exon 3, *EMC7* exon 5, *GAPDH* E1-E2-E3, *GPI* exon 4, *GPI* exon 6, *MRPL19*, *OAZ1* E2-E3, *POLR2A* E20-21, *RPL19*, *RPLP0*, *SF3A1*, *TBP*, *TUBB*, *c1orf43* exon 2), according to nCounter Expression Data Analysis Guide (mAN-C0011-02). Finally, they were log2-transformed and centered around the mean. All data was analyzed with R/Bioconductor (v3.6.3/v2.46.0). Any sample with a mean of

less than 3000 total counts (pre-normalization) of the 19 probes was excluded. Missing values were imputated with knn algorithm. The routine percentage of failure is 4.2% for nCounter (Nanostring) profiling. Using the 3000 counts threshold, no significant differences were observed in the 10 most common tumor histologies for nCounter profiling failure (p = 0.5) (Chi-square test).

Histopathologic analysis of the proportion of stromal tumor infiltrating lymphocytes (TILs) was done in whole sections of tumor tissue stained with hematoxylin and eosin (H&E). TILs were quantified according to recommendations developed by the International TILs Working Group.[57–59]

VIGex 12-gene signature score for each sample was computed as follows:

$$\sum_{i-1}^{12}\left(\log 2\left(expr.gene_i\right) - average\left(\log 2\left(expr.gene_i \text{ in training dataset}\right)\right)\right)$$

With the 12-selected genes: *CTLA-4*, *CD274*, *PCDC1*, *IL7R*, *FOXP3*, *CXCL9*, *CXLX10*, *CXCL11*, *IFNG*, *PRF1*, *GZMA* and *GZMB*.

VIGex inter-laboratory validation

RNA libraries were prepared at Princess Margaret Cancer Center using the Illumina Stranded Total RNA Prep Ligation with Ribo-Zero Plus and sequenced using 100bp paired end chemistry on Illumina Novaseq6000. FASTQs were aligned to the hg38 human reference genome using STAR 2.7.2b aligner with default settings.[60] Expression levels of all transcripts were quantified using RSEM 1.3.0[61] and annotated with GENCODE transcript reference version 31. Counts from Princess Margaret Cancer Center dataset and the VHIO dataset were normalized with DESeq2 and transformed to log2 values. Samples from the VHIO dataset were used as training dataset for the calculation of VIGex Score of the samples from Princess Margaret Cancer Center. Finally, the parameters of a linear regression between the Nanostring-VIGex scores and RNA-VIGex scores of the samples from VHIO dataset were used to calibrate the VIGex Scores. VIGex scores were used to categorize samples into Hot (VIGex score >0.75), I-Cold (VIGex score between −0.75 and 0.75) and Cold groups (VIGex score <(-0.75)).

Publicly available datasets of patients treated with immunotherapy in the metanalysis

Metanalysis studies were identified by performing a systemic review on PubMed using the MeSH terms: (cancer OR tumor) AND ((PD-1 OR PD1) OR (PD-L1 OR PDL1) OR (CTLA-4 OR CTLA4)) AND ((anti-PD-1 OR anti-PD1) OR (anti-PD-L1 OR anti-PDL1) OR (anti-CTLA-4 OR anti-CTLA4)) AND (genomic OR transcriptomic OR mutation) as previously reported.[62] Eligible studies were English language, including at least one type of genomic data and clinical outcome information from advanced solid tumor patients treated with anti-PD1/PD-L1 and/or anti-CTLA-4 antibodies, and were published between January 2015 and September 2020. Genomic data was defined as RNA-sequencing and/or tumor exome or targeted-DNA sequencing. Clinical outcome data included response (according to RECIST or other response criteria), PFS, or OS. Studies with fewer than 20 patients were excluded. Trials of IO in combination with other treatment modalities such as chemotherapy, targeted therapies, and radiation were excluded. There was no minimum duration of follow-up for inclusion. Trials in the neoadjuvant setting were excluded.

Outcome data, mutational and transcriptomic profiles were collected for each study. If not publicly available, individual patient clinical and molecular data information

were requested from the corresponding authors. The processed transcriptomic profile, composed of log2-transformed TPM (Transcripts Per Million) data. When raw sequencing data were available (Fumet.1,[34] Fumet.2,[34] Hugo,[14] Hwang,[35] Jung[36] and Riaz[37]), transcripts abundance was quantified from the fastq files through Salmon (v1.4.0),[63] using the grch38 GENCODE transcriptome of reference. Gene-level TPM data was then obtained from the estimated transcript abundance level with tximport (v.1.20.0) R package. Otherwise, raw count/TPM data were downloaded directly from the respective publications (Braun,[38] Liu,[39] Mariathasan,[40] Miao.1,[41] Snyder,[42] Van_Allen[43]). FPKM (Fragments Per Kilobase of transcript per Million mapped reads) from Nathanson[44] was converted to TPM data using this formula:

$$TPM_I = \left(\frac{FPKM_I}{\sum_J FPKM_J}\right) \times 10^6$$

For each dataset, genes with zero expression value in at least 50% of the samples were filtered out. Because of the presence of variability in clinical follow-up between studies, OS and PFS were censored, respectively, at 36 and 24 months.

VIGex and tumor mutational burden computation in the metanalysis

The 12-gene VIGex gene signature for the metanalysis was computed using Gene Set Variation Analysis (GSVA)[64] enrichment score. For each investigated study, signatures were only computed if at least 80% of their genes were present in the data. We applied *Z* score transformation to the genes of each signature before the computation. *Z* score transformation was applied before the GSVA or the weighted mean computation and after the computation. The computation of the TMB per megabase (Mb) was performed as defined: $TMB = mut_{ns}/target$. With mut_{ns} and *target* defined, respectively, as the number of non-synonymous mutations and the target size of the sequencing.

QUANTIFICATION AND STATISTICAL ANALYSIS

Clinical benefit (CB) was defined as RECIST (v1.1) complete (CR) or partial (PR) response or stable disease (SD) without a PFS event at 6 months. No clinical benefit was defined as RECIST progressive disease (PD) or RECIST SD with a PFS event occurring within 6 months. PFS was calculated from first IO treatment until progressive disease by RECIST 1.1, death or loss of follow up. OS was calculated from first dose of IO until death or loss of follow up. Specifically, for the metanalysis of publicly available datasets, if RECIST information was not available, patients without any PFS event at 6 months and patients with a PFS event occurring within 6 months were classified as CB and no-CB, respectively.[62] If PFS information was unavailable, patients with RECIST SD as best response were classified as non-evaluable. Survival analysis were done with survival R package and using Cox Proportional Hazards method.[65] Differences between two-continuous variables were assessed using Wilcoxon test or t-test. Fisher's exact test or Chi-square test were used to assess statistical significance between categorical variables. Association of specific biomarkers with clinical benefit was assessed using a logistic regression model.

For the metanalysis, the results of individual independent studies were pooled using random-effects metanalysis with inverse variance weighting in DerSimonian and Laird random-effects models.[66] Heterogeneity across studies was evaluated by using the Q statistic along with I^2 index, which describes the total variation across studies attributable to heterogeneity rather than sampling error.[67–69] Note that I^2 value of greater than 50% along with Cochran's Q statistic $P < 0.05$ represent moderate to high heterogeneity.[67] Subgroup analysis was considered to assess the

impact of tumor type, sequencing technology and normalization method on the source of moderate to high heterogeneity.[66] Potential publication bias was performed using the funnel plot and the Egger test. No statistically significant publication bias was observed (data not shown). All analyses were performed on the R platform (version 3.6.3). When needed p values were corrected for multiple testing using the Benjamini-Hochberg (False Discovery Rate, FDR) method. Associations were deemed statistically significant for p values and/or FDR lower or equal to 0.05.